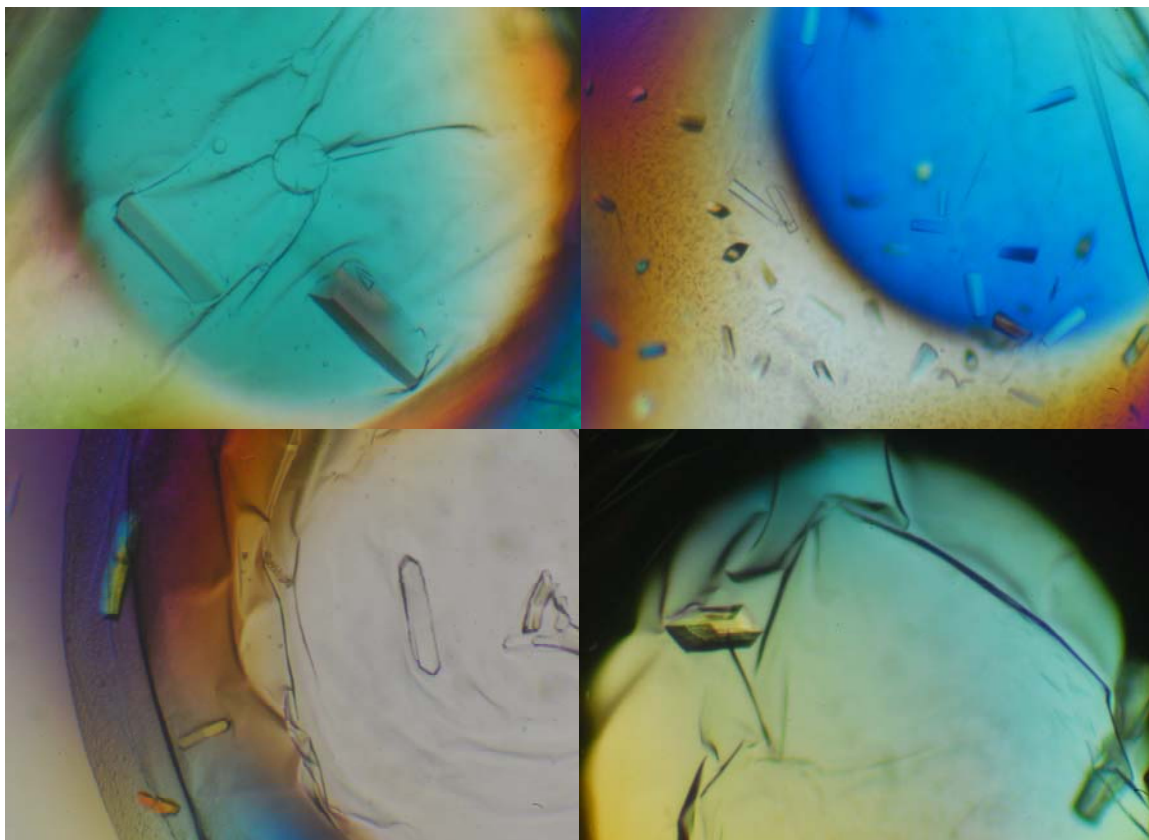


A structural study on the Alzheimer's disease amyloid β peptide



Date: June 12, 2008
Name: Maria Koster
Student number: 1223626
School: Hogeschool Utrecht, Life Sciences & Chemistry
Major: Molecular Biology
Internship location: Texas A&M University
Department of Biochemistry & Biophysics
College Station, Texas, USA
Period: September 1st 2007 till May 31st 2008
Supervisors: Dr. J. C. Sacchettini
J. Mire
Mentor: Dr. M. F. van Berlo

Preface

From September 2007 till May 2008 I have done an internship in the Sacchettini Lab in the Department Biochemistry and Biophysics of Texas A&M University in College Station. There are no words for how much I have learned and experienced during this period in my life, on a professional as well as personal level. I can truly say that it has been an amazing and unforgettable experience.

Of course this internship would not have been possible without the help and effort of others. I would like to thank Dr. James Sacchettini for giving me the opportunity to work in his lab. I would like to thank Joseph Mire for teaching and guiding me, thank you so much! Further I would like to thank Dr. Mario van Berlo for helping me to find this internship place. Last but not least I want to thank all the people in the lab. Everybody has been so helpful and nice to me; it made me feel like being at home. I will never forget you guys. I wish you all the best in life!

Maria Koster

College Station, May 2008

Summary

Alzheimer's disease (AD) is a neurodegenerative disease. The disease is characterized by the presence of neuropathology hallmarks such as: senile plaques, neurofibrillary tangles and the loss of synapses and neurons in the brain. The senile plaques are mainly composed of amyloid fibrils of the protein amyloid β ($A\beta$)^{4,5}.

$A\beta$ arises naturally in the human brain throughout life as a result of metabolic processing of the amyloid precursor protein (APP)¹². There are several $A\beta$ peptides, which originate after cleavage of APP. The 42 residue long peptide, $A\beta_{42}$ is the major component of the senile plaques in AD¹⁵. Alzheimer's disease is thought to develop through a process called amyloid cascade where an increase of $A\beta$ level results in oligomerization and aggregation of $A\beta_{42}$ thereby triggering a downstream cascade of pathological events³.

More and more evidence indicates that especially the soluble $A\beta$ oligomers (that are assemblies of the $A\beta$ monomer) are neurotoxic and play an important role in the AD related pathology^{4,5,23,25}.

The ultimate aim of this study was to solve the structure of $A\beta_{42}$ in an oligomeric state for rational structure based drug design against Alzheimer's disease. Protein purification and X-ray crystallography techniques were used. $A\beta$ was linked to the apical domain of the chaperonin protein GroEL and the fusion protein ApicalGroEL- $A\beta$ was created. This fusion inhibited the rapid fibrillization of $A\beta$, thereby forming the possibility to trap $A\beta$ in an oligomeric state. Eleven different constructs were made. They contained a N-terminal His-tag followed by the apical domain of GroEL. In between the apical domain and $A\beta$ different synthetic sequences, the so-called linkers were placed to manipulate the arrangement of $A\beta$. Also, different size combinations of the apical domain of GroEL and $A\beta$ were tested.

The ApicalGroEL- $A\beta$ constructs were expressed and purified and two different crystallization approaches were used. The first approach was to isolate the protein as a monomer and screen for crystallization. Since $A\beta$ has the propensity to form oligomers when it is at a high enough concentration¹⁷, the assumption was made that the protein would oligomerize in the crystal. The second approach was to isolate ApicalGroEL- $A\beta$ in an oligomeric state and to crystallize the protein in this oligomeric state. The protein monomer was purified, brought to high concentration and incubated to see if it would form oligomers in a time dependent manner, which could then be purified and crystallized.

Structures of three different ApicalGroEL- $A\beta$ constructs in a monomeric state were solved. The electron density maps showed electron density for the apical domain of GroEL, up to the last residue. No connected and continuous electron density was present for the linker and $A\beta$. Further analysis suggested that $A\beta$ is present in the crystals. The missing electron density could have been due to too much flexibility of $A\beta$ in the unit cell. It could also be due to a disordered conformation of $A\beta$ itself.

The ApicalGroEL- $A\beta$ monomer oligomerizes in a time dependent manner. No attempt was made yet to isolate and crystallize these oligomers. The best approach would be to

isolate and crystallize the smaller size oligomers (dimers and trimers) since these are stable^{23,24}.

Linking A β to the apical domain of GroEL offers advantages; the ApicalGroEL-A β protein is soluble and easy to purify and crystallize. In addition the apical domain of GroEL itself does not oligomerize, therefore a stable oligomer formed is due to the presence of A β .

Unfortunately it was not possible to solve an oligomer structure of A β yet. However there are still multiple approaches that can be tried, hopefully one of them will eventually enable us to solve the structure of A β in an oligomeric state. Thereby making it possible to design drugs that specifically target A β oligomers and help to win the fight against Alzheimer's disease.

Samenvatting

De ziekte van Alzheimer (AD) is een neurodegeneratieve ziekte. De ziekte wordt gekarakteriseerd door de aanwezigheid van neuropathologische kenmerken waaronder: plaques, neurofibrillaire knopen en de afname van synapsen en neuronen in de hersenen. De plaques bestaan voornamelijk uit amyloïde fibrillen van het eiwit amyloid β ($A\beta$)^{4,5}.

$A\beta$ komt van nature voor in de humane hersenen tijdens het leven en ontstaat door metabole verwerking van het amyloïd voorloper eiwit (APP)¹². Er zijn verscheidene $A\beta$ peptides die ontstaan na klieving van APP. De 42 residu lange peptide, $A\beta_{42}$ is de voornaamste component in de plaques in AD¹⁵. De ziekte van Alzheimer ontwikkelt zich waarschijnlijk via de zogenaamde amyloïde cascade waarbij een toename van $A\beta$ leidt tot oligomerizatie en aggregatie van $A\beta_{42}$ wat een cascade van pathologische gebeurtenissen tot gevolg heeft³.

Steeds meer bewijs wijst er op dat voornamelijk de oplosbare $A\beta$ oligomeren (dat zijn verzamelingen van $A\beta$ monomeren) neurotoxisch zijn en een belangrijke rol spelen in de AD gerelateerde pathologie^{4,5,23,25}.

Het doel van deze studie is het bepalen van de structuur van $A\beta_{42}$ in een oligomerische vorm, voor op structuur gebaseerde medicijnontwikkeling gericht tegen de ziekte van Alzheimer. Technieken zoals eiwitzuivering en röntgenstraling crystallografie werden toegepast. $A\beta$ werd gelinkt aan het apicale domein van het chaperonine eiwit GroEL waarbij het fusie-eiwit ApicalGroEL- $A\beta$ werd gecreëerd. Deze fusie voorkomt snelle fibrillizatie van $A\beta$, hierdoor wordt de mogelijkheid gevormd om $A\beta$ te vangen in een oligomerische vorm. Elf verschillende constructen zijn gemaakt. Ze hadden een N-terminale His-tag gevolgd door het apicale domein van GroEL. Tussen het apicale domein van GroEL en $A\beta$ zijn verschillende synthetische sequenties, de zogenaamde linkers geplaatst om de ordening van $A\beta$ te manipuleren. Daarnaast zijn verschillende combinaties in grootte van het apicale domein van GroEL en $A\beta$ uitgetest.

De ApicalGroEL- $A\beta$ constructen werden tot expressie gebracht en gezuiverd. Vervolgens zijn twee verschillende kristallisatiebenaderingen toegepast. $A\beta$ heeft de neiging om oligomeren te vormen als de concentratie hoog genoeg is¹⁷, daarom werd aangenomen dat het eiwit zou oligomerizeren in de kristal. De tweede benadering was het isoleren en kristalliseren van ApicalGroEL- $A\beta$ in een oligomerische vorm. De eiwit monomeer werd gezuiverd en tot hoge concentratie gebracht. Vervolgens werd het geïncubeerd over een periode om te zien of het oligomeren zou vormen die gezuiverd en gekristalliseerd konden worden.

De structuur van drie verschillende ApicalGroEL- $A\beta$ constructen in een monomerische vorm zijn bepaald. De 3D afbeelding van de electronendichtheid liet electronendichtheid voor het apicale domein van GroEL zien tot en met de laatste residu. Geen aaneengesloten en continue electronendichtheid was aanwezig voor de linker en $A\beta$. De niet aanwezige electronendichtheid kan het gevolg zijn van een te grote flexibiliteit van $A\beta$ in de eenheidscel. Het kan ook een gevolg zijn van dat $A\beta$ zich in een ongeordene conformatie bevond.

De ApicalGroEL- $A\beta$ monomeer oligomeriseert na een incubatieperiode. Het is nog niet

gepoogd om deze oligomeren te isoleren en kristalliseren. De beste benadering zou het isoleren en kristalliseren van de kleinere oligomeren (dimeren en trimeren) zijn aangezien deze stabiel zijn^{23,24}.

Het linken van A β aan het apicale domein van GroEL biedt voordelen; het ApicalGroEL-A β eiwit is oplosbaar en gemakkelijk te zuiveren en kristalliseren. Ook oligomeriseert het apicale domein van GroEL niet uit zichzelf, elk stabiel gevormde oligomeer is daarom afhankelijk van de aanwezigheid van A β .

Helaas was het niet mogelijk om een oligomeerstructuur van A β te bepalen. Er zijn nog verschillende benaderingen die uitgeprobeerd kunnen worden, hopelijk zal een van deze het mogelijk maken op de structuur van A β in een oligomerische vorm te bepalen. Daarmee zou de mogelijk gecreëerd worden om medicijnen te ontwikkelen die zich specifiek richten op A β oligomeren. Dit kan helpen om het gevecht tegen de ziekte van Alzheimer te winnen.

Abbreviations

Å	Ångstrom
A β	Amyloid beta
AD	Alzheimer's disease
AICD	APP intracellular domain
APP	Amyloid precursor protein
AU	Absorbance unit
BACE	β -site APP cleavage enzyme
CTF	C-terminal fragment
DLS	Dynamic light scattering
DS	Down Syndrome
FPLC	Fast protein liquid chromatography
GAG	Glycosaminoglycan
IPTG	Isopropyl- β -thiogalactopyranoside
LB	Luria-Bertani
LTP	Long-term potentiation
mQ	MilliQ water
Mw	Molecular weight
NCT	Nicastrin
NFT	Neurofibrillary tangle
NTF	N-terminal fragment
O.D.	Optical density
PDB ID	Protein Data Bank identification
PMSF	Phenylmethanesulfonyl fluoride
PS	Presenilin
qHX-NMR	Quenched hydrogen-exchange nuclear magnetic resonance
ssNMR	Solid state nuclear magnetic resonance
U	Unit

PREFACE	3
SUMMARY	4
SAMENVATTING	6
ABBREVIATIONS	8
CHAPTER 1; INTRODUCTION	12
1.1 BIOCHEMICAL BACKGROUND OF AMYLOID BETA.....	12
1.1.1 <i>Amyloid diseases</i>	12
1.1.2 <i>Alzheimer's disease</i>	12
1.1.3 <i>Amyloid beta discovery and formation process</i>	13
1.1.4 <i>Amyloid beta fibrillization process</i>	14
1.1.5 <i>Amyloid beta oligomer pathology</i>	15
1.1.6 <i>Amyloid beta oligomer kinetics</i>	16
1.1.7 <i>Common fibril and oligomer structures of amyloids</i>	17
1.1.8 <i>Amyloid beta proposed structures</i>	18
Conformation transition from α -helical to β -sheet.....	18
Amyloid beta monomer α -helical structures in apolar solution.....	19
Amyloid beta monomer collapsed coil structure in polar solution.....	19
Amyloid beta fibril β -sheet structures	19
1.1.9 <i>Drugs against Alzheimer's disease</i>	20
1.2 PROTEIN CRYSTALLOGRAPHY.....	21
1.2.1 <i>Crystallization</i>	21
1.2.2 <i>X-ray diffraction</i>	22
1.2.3 <i>The phase problem</i>	23
1.2.4 <i>Model building</i>	23
1.3 AIM AND PROCEDURE	24
CHAPTER 2; MATERIALS AND METHODS	27
2.1 GENERAL EXPERIMENTS: PLASMID, GENE AND PROTEIN CONSTRUCTS.....	27
2.2 GENERAL EXPERIMENTS: CLONING OF THE APICALGROEL-A β CONSTRUCTS.....	28
2.2.1 <i>Plasmid preparation</i>	28
Double digestion.....	28
DNA extraction from agarose gel.....	28
2.2.2 <i>Insert preparation</i>	29
Linker preparation	29
Gene preparation.....	29
2.2.3 <i>Ligation and transformation</i>	30
Linker ligation into cut plasmid	30
Gene ligation into cut plasmid.....	30
Plasmid transformation into NovaBlue competent cells.....	31
2.2.4 <i>ApicalGroEL-Aβ construct confirmation</i>	31
Overnight cultures	31
Plasmid isolation.....	31
PCR to confirm construct.....	31

Sequencing to confirm construct	32
2.3 GENERAL EXPERIMENTS: EXPRESSION OF THE APICALGROEL-A β CONSTRUCTS	32
2.3.1 Plasmid transformation into BL21 competent cells	32
2.3.2 Expression test	32
2.4 GENERAL EXPERIMENTS: APICALGROEL-A β PURIFICATION	33
2.4.1 Cell growth and protein production	33
2.4.2 Cell lysis	33
2.4.3 Nickel affinity chromatography	33
2.5 APICALGROEL-A β ISOLATION AS A MONOMER	34
2.5.1 Crystallization preparation	34
2.5.2 Crystallization screening	34
2.5.3 Crystallization optimization	35
2.5.4 Structure determination and refinement	35
2.5.5 Monomer cleavage analysis	35
Mass spectrometry	35
2.5.6 Crystal composition analysis	35
2.6 APICALGROEL-A β ISOLATION AS AN OLIGOMER	36
2.6.1 Time dependent oligomerization analysis	36
Superdex 75 size exclusion chromatography	36
Room temperature incubation	36
Dynamic light scattering	37
Western blotting	37
2.7 THE HIGHER MOLECULAR WEIGHT PROTEIN	37
2.7.1 Non-specific protein or an ApicalGroEL-A β oligomer	37
Western blotting	37
2.8 GENERAL TECHNIQUES, MEASUREMENTS AND PREPARATIONS	37
2.8.1 DNA separation by agarose gel	37
2.8.2 Protein separation by SDS-PAGE	38
2.8.3 Western blot analysis	38
2.8.4 DNA concentration measurement	39
2.8.5 Protein concentration measurement	39
2.8.6 Bacterial growth measurement	39
2.8.7 LB agar plates	39
2.8.8 LB cultures	39
2.8.9 LB media	40
2.9 APPARATUS	40
CHAPTER 3; RESULTS	41
3.1 GENERAL RESULTS	41
3.1.1 Cloning of the ApicalGroEL-A β constructs	41
3.1.2 Expression of the ApicalGroEL-A β constructs	41
3.1.3 Purification of the ApicalGroEL-A β constructs	42
3.2 APICALGROEL-A β ISOLATION AS A MONOMER	43
3.2.1 Crystallization	43
3.2.2 Solved structures	44
A376-6SAG-A β 42 structure 1	44

A376-6SAG-A β 42 structure 2.....	45
A376-6MPT-A β 42 structure	46
A376-6SAG-A β 17-42 structure	47
3.2.3 <i>Monomer cleavage analysis</i>	47
Mass spectrometry	47
Western blotting	48
3.2.4 <i>Crystal composition analysis</i>	48
Western blotting	48
3.3 APICALGROEL-A β ISOLATION AS AN OLIGOMER.....	49
3.3.1 <i>Time dependent oligomerization analysis</i>	49
Dynamic light scattering	49
Western blotting	50
3.4 THE HIGHER MOLECULAR WEIGHT PROTEIN	51
3.4.1 <i>Non-specific protein or an ApicalGroEL-Aβ oligomer</i>	51
SDS-PAGE analysis	51
Western blotting	52
CHAPTER 4; DISCUSSION AND CONCLUSION	53
4.1 APICALGROEL-A β ISOLATION AS A MONOMER	53
4.2 APICALGROEL-A β ISOLATION AS AN OLIGOMER.....	54
4.3 THE HIGHER MOLECULAR WEIGHT PROTEIN	54
4.4 SUGGESTIONS FOR FURTHER RESEARCH.....	54
4.5 CONCLUDING STATEMENT.....	55
REFERENCES.....	56
WEBSITES.....	59
SUPPLEMENTS	60
SUPPLEMENT 1 AMYLOID BETA PEPTIDE FRAGMENT STRUCTURES.....	60
SUPPLEMENT 2 GROEL BACKGROUND INFORMATION.....	62
SUPPLEMENT 3 CHROMATOGRAM OF A NICKEL COLUMN PURIFICATION.....	63
SUPPLEMENT 4 DYNAMIC LIGHT SCATTERING ANALYSIS.....	64
SUPPLEMENT 5 SDS-PAGE OF A SIZE EXCLUSION PURIFICATION.....	65
SUPPLEMENT 6 PRIMER NUCLEOTIDE SEQUENCES	66
SUPPLEMENT 7 LINKER NUCLEOTIDE SEQUENCES	68
SUPPLEMENT 8 AMINO ACIDS SEQUENCE CONSTRUCTS	70

Chapter 1; Introduction

1.1 Biochemical background of amyloid beta

1.1.1 Amyloid diseases

Protein misfolding diseases arise from the failure of a protein to adopt or remain in its native biological conformation. These incorrectly folded proteins often self-associate to form an aggregate, which can lead to the so-called aggregation diseases. There are approximately forty known aggregation diseases that result in amyloid formation, which is known as an amyloid disease or amyloidosis. The aggregation can occur in one single type of tissue or in multiple types of tissues. Amyloids are extracellular deposits of insoluble fibrils in organs and tissues. They bind the dye Congo red and give a green birefringence under a polarization microscope after Congo red staining. Congo red recognizes the β -pleated structure found in the fibrils, this is not well understood. Some amyloid diseases are: Parkinson's disease, Huntington's disease, Type II diabetes and the most well-known and well-studied Alzheimer's disease (AD). In AD, aggregation and deposition of the protein amyloid β ($A\beta$) takes place in the human brain as extracellular senile plaques (Fig. 1-1)¹⁻³.

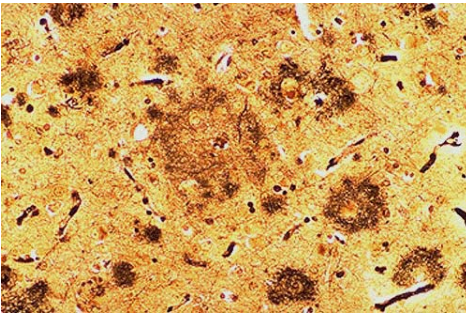


Figure 1-1 Senile plaques in Alzheimer's disease. Seen with a silver stain⁴³.

Alzheimer's disease is a neurodegenerative disease of the central nervous system. The first case was presented by the psychiatrist Alois Alzheimer in 1906. Now more than 30 million people worldwide are affected with AD⁴. Alzheimer's disease patients experience gradual memory loss (dementia) and other declines in cognitive function. The disease is characterized by the presence of neuropathology hallmarks such as: senile plaques, intraneuronal neurofibrillary tangles (NFTs) and the loss of synapses and neurons in the brain. Neurofibrillary tangles are composed of aggregated hyperphosphorylated protein tau. Whereas extracellular plaques are mainly composed of amyloid fibrils of the protein amyloid β ($A\beta$) (Fig. 1-1). Although amyloid β arises naturally in the human brain throughout life, it seems to play a central role in the pathogenesis of AD^{4,5}. The neurotoxic species of $A\beta$ was long thought to only be the insoluble fibrillar form found in extracellular plaques in AD brain. However, it was observed that the plaques are more prevalent with age in AD patients and they are also

1.1.2 Alzheimer's disease

Alzheimer's disease is a neurodegenerative disease of the central nervous system. The first case was presented by the psychiatrist Alois Alzheimer in 1906. Now more than 30 million people worldwide are affected with AD⁴. Alzheimer's disease patients experience gradual memory loss (dementia) and other declines in cognitive function. The disease is characterized by the presence of neuropathology hallmarks such as: senile plaques, intraneuronal neurofibrillary tangles (NFTs) and the loss of synapses and neurons in the brain. Neurofibrillary tangles are composed of aggregated hyperphosphorylated protein tau. Whereas extracellular plaques are mainly composed of amyloid fibrils of the protein amyloid β ($A\beta$) (Fig. 1-1). Although amyloid β arises naturally in the human brain throughout life, it seems to play a central role in the pathogenesis of AD^{4,5}. The neurotoxic species of $A\beta$ was long thought to only be the insoluble fibrillar form found in extracellular plaques in AD brain. However, it was observed that the plaques are more prevalent with age in AD patients and they are also

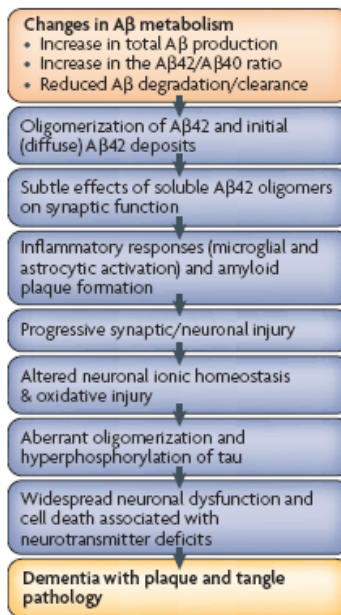


Figure 1-2 Amyloid cascade³.

found in cognitively normal individuals. In addition to that the number of plaques in the brain seemed to roughly correlate with the severity of the disease^{6,7}. Also, soluble A β in the brain is shown to be much better correlate with the severity of the disease. Soluble A β has the potential to do harm over a much wider area than insoluble A β due to insoluble A β being fixed to one single location while soluble A β is able to freely diffuse into the synaptic cleft^{8,9}.

This suggests a neurotoxic role for the soluble A β content in the brain. It is not known which assemblies of A β are pathogenic, although more and more is becoming clear. The disease is thought to develop through a process called amyloid cascade (Fig. 1-2) where an increase of A β level results in oligomerization and aggregation of A β _{residues 1-42} (A β ₄₂) and thereby triggering a downstream cascade of pathological events³. The deposition of the protein tau intraneuronal as NFTs is believed to be a downstream event in the amyloid cascade⁴.

1.1.3 Amyloid beta discovery and formation process

The link of A β with Alzheimer's disease was first made by Glenner and Wong (1984). They were the first to discover that the amyloid fibrils found in the brains of AD patients are mainly composed of a 4.5 kDa protein that they named amyloid fibril protein β ¹⁰. The gene encoding for the precursor of amyloid β , amyloid precursor protein (APP) (an integral membrane protein) is located on chromosome 21¹¹.

A β arises naturally in the human brain throughout life as a result of metabolic processing of the amyloid precursor protein (APP). APP is expressed in many tissues, both neural and nonneural, with high expression in the brain¹². There are two competing pathways that can process APP. In the non-amyloidogenic pathway APP is cleaved by the protease α -secretase that cleaves APP in the middle of A β and thus prevents A β generation. In the amyloidogenic pathway APP is cleaved by the proteases β - and γ -secretase, which eventually results in liberation of the A β peptide into the extracellular space^{13,14}.

When APP is cleaved via the amyloidogenic pathway it is first cleaved by β -secretase (also known as β -site APP cleaving enzyme: BACE), resulting in secretion of the ectodomain (Fig. 1-3 A). Next an intramembrane cleavage takes place, which is mediated by the γ -secretase complex (Fig. 1-3 B). After the BACE cleavage the remaining membrane part of APP (CTF β) is transferred to the active site of the γ -secretase complex, in between the transmembrane domains 6 and 7 of presenilin-1 (PS1) or PS2. PS1 and PS2 are autoproteases, after cleavage their N- and C-terminal fragments are created (NTF and CTF). In addition to PS1 and PS2, three other proteins make part of the γ -secretase complex; nicastrin (NCT), APH1 and PEN2. The γ -secretase complex cleaves CTF β at multiple sites (Fig. 1-3 C). The γ -secretase complex ϵ -cleavage releases the APP intracellular domain (AICD) into the cytosol (Fig. 1-3 B, C and D). The remaining membrane fragment is next cut at the ζ -site and at last at the γ -site which releases A β into the extracellular space (Fig. 1-3 B, C and D)³. The γ -cleavage site is variable; it happens after amino acid 38, 40 or 42, producing different lengths of full-length A β peptides (39-43 amino acids) (Fig 1-3 C and D), which has a large influence on the pathogenicity of A β ³.

The 40 residue peptide, A β ₄₀ is the major A β peptide found in the cerebrospinal fluid (90 %), while the 42 residue peptide, A β ₄₂ is the major component of the plaques in AD (see Fig. 1-4 for the amino sequence of full-length A β peptides)¹⁵. A β ₄₂ is much more pathogenic than A β ₄₀. It is more hydrophobic compared to A β ₄₀ because of its two extra C-terminal residues; alanine and isoleucine (Fig. 1-4). It therefore aggregates more rapidly and forms stable oligomers faster and easier than A β ₄₀. Because of these properties, A β ₄₂ is thought to be more pathogenic and amyloidogenic than A β ₄₀³. Imbalance between the A β production and clearance resulting in oligomerization and aggregation of A β ₄₂ into plaques is thought to be an important event in AD. More than a hundred mutations in the gene encoding for the precursor of A β , APP and mutations in genes encoding for PS1 and PS2 have been found to cause AD. These mutations increase the production of A β and especially the more amyloidogenic A β ₄₂³.

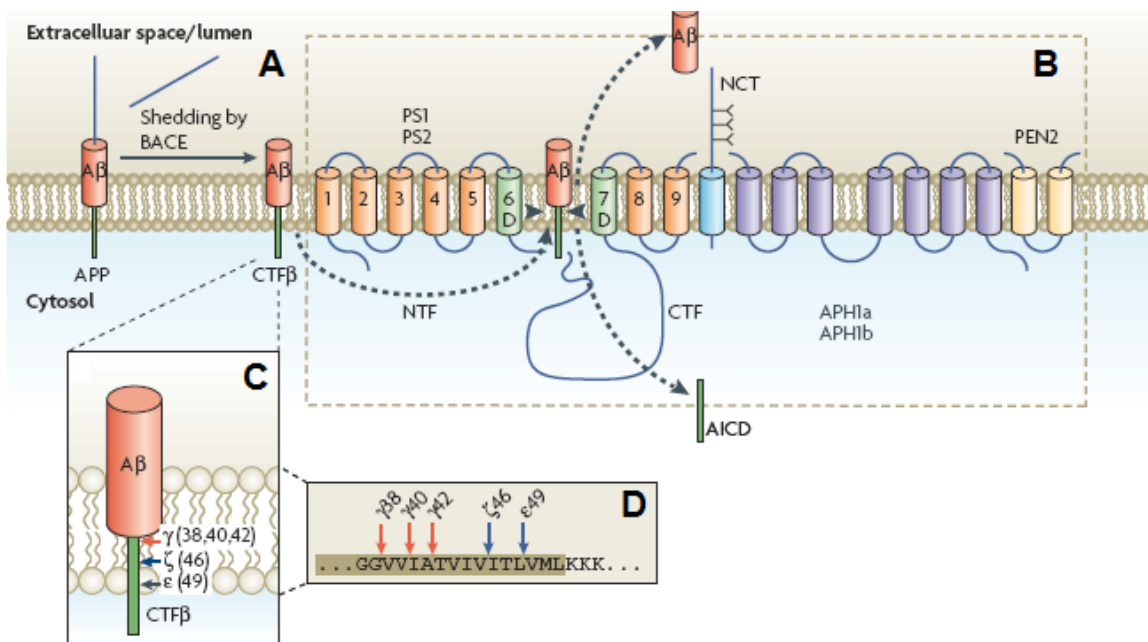
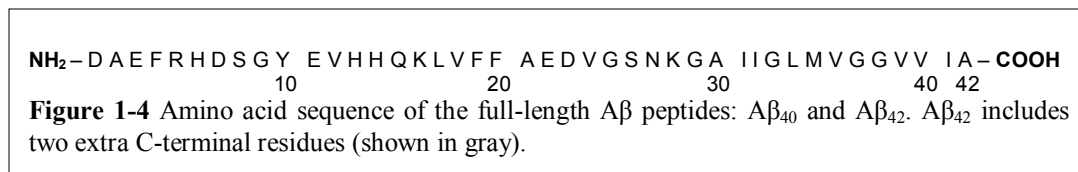


Figure 1-3 Amyloid β generation by metabolic processing of the amyloid precursor protein³.



1.1.4 Amyloid beta fibrillization process

There are multiple A β assemblies that can be divided into two distinct categories: fibrillar and non-fibrillar. The non-fibrillar A β assemblies include the A β monomer and small soluble oligomers; soluble oligomers are assemblies of A β monomers. The fibrillar A β assemblies include protofibrils and fibrils.

The A β monomer has an α -helical structure in membrane-like conditions and adopts an unordered conformation (collapsed coil) in aqueous solution (section 1.1.8). In contrast

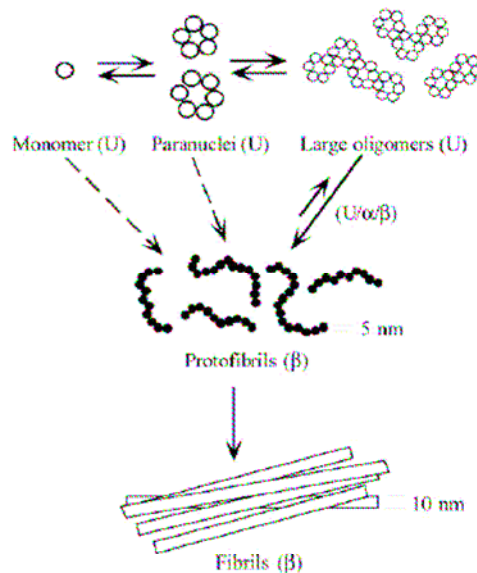


Figure 1-5 A β_{42} assembly model. Monomers assemble into paranuclei that assemble further to form large oligomers. Monomers, paranuclei and large oligomers are predominately unstructured. Protofibril may form from large oligomers. There are two alternative pathways in which direct addition of monomers or paranuclei to protofibrils is suggested (dotted arrows). Protofibrils mature into insoluble fibrils. α = helical elements. β = β -sheet/ β -turn U = unstructured¹⁹.

A β in fibrils has a β -sheet structure (section 1.1.8). Therefore a conformational change to the β -sheet structure is thought to result into fibril formation¹⁶.

Monomers assemble rapidly to form oligomers and equilibrium is formed¹⁷. Once the oligomers are starting to interact slowly to form higher order assemblies such as paranuclei (spherical oligomers) and large oligomers, protofibrils are formed; small elongated A β oligomers with β -sheet structure (Fig. 1-5)¹⁸. The protofibril formation is reversible on dilution; a protofibril can depolymerize into oligomers and monomers. Thus equilibrium is formed between protofibrils and oligomers. Protofibrils mature into insoluble fibrils with β -sheet structure¹⁹. The formation of fibrils is irreversible; once it is formed it is not easily degraded into lower order species even when diluting the fibrils⁷.

It is not completely clear how fibril formation occurs. There is evidence that oligomer formation is not even necessary for fibrillization, suggesting that oligomer and fibril formation are two distinct pathways¹⁷.

Fibrils can be composed of A β_{40} as well as

A β_{42} , but are mainly composed of A β_{42} . The much higher propensity of A β_{42} to aggregate into insoluble fibrils compared to A β_{40} is due to the two extra C-terminal amino acids in A β_{42} . These two amino acids appear to be important for fibril formation kinetics²⁰.

1.1.5 Amyloid beta oligomer pathology

Intraneuronal accumulation of A β precedes the appearance of senile plaques and NFT's (Fig. 1-2). The intracellular A β is neurotoxic and affects synaptic function. The intracellular A β consists of monomers and oligomers²¹. A large variety of A β oligomer sizes have been found in *in vivo* and *in vitro* studies (Tab. 1-1). Oligomer size distributions of A β_{40} and A β_{42} are shown to be distinct, large oligomers are only observed for A β_{42} ¹⁹. It is unclear what size A β oligomers exist *in vivo* and which ones are pathological. However, there are studies pointing towards toxicity of specific oligomeric states.

The neurotoxicity of soluble A β_{42} was determined in an *in vitro* study where synthetic A β_{42} (forming monomer as well as oligomer assemblies) was injected into the cytoplasm

of cultured primary human neurons and caused significant cell death. A β_{40} was significantly less toxic and the toxicity of A β_{42} was proven to be selective for neurons²². One of the studied neuropathological events caused by human A β oligomers is the blocking of hippocampal long-term potentiation (LTP) in rats. LTP is blocked in rats *in vivo* when the oligomers are injected into the hippocampus. LTP is considered to be an important mechanism for learning and memory. It is possible that the memory decline seen in AD is a result of similar LTP impairment as is caused by A β oligomers seen in rats²³.

In vitro experiments on mice hippocampal brain slices showed the strongest LTP inhibition caused by A β trimers and a lower inhibition caused by dimers and tetramers⁴. In contrast to the oligomer assemblies, both the above *in vivo* and *in vitro* studies show that monomeric A β does not affect LTP. Suggesting a pathological role for A β oligomer assemblies.

A specific oligomeric state that was found to be toxic in an *in vivo* study is a dodecamer. In transgenic mice memory impairment is shown to be correlated with accumulation of an extracellular 56 kDa oligomer (A β *56) (dodecamer). Purified A β *56 from mice brains disrupts memory when injected into the brains of rats²⁴.

Oligomer assembly	Origin
Dimer: A β_{40} and A β_{42}	Synthetic ¹⁹ In vivo human ²⁵ In vitro ^{4,23,25,26}
Trimer: A β_{40} and A β_{42}	Synthetic ¹⁹ In vitro ^{4,23,25,26} In vivo transgenic mice ²⁴
Tetramer: A β_{40} and A β_{42}	Synthetic ^{4,19}
Pentamer: A β_{42}	Synthetic ¹⁹
Hexamer: A β_{42}	Synthetic ¹⁹ In vivo transgenic mice ²⁴
Octamer: A β_{42}	Synthetic ¹⁹
Nonamer: A β_{42}	Synthetic ¹⁹ In vivo transgenic mice ²⁴
Dodecamer: A β_{42}	Synthetic ^{19,27} In vivo transgenic mice ²⁴ In vivo human ²⁷
Octadecamer: A β_{42}	Synthetic ¹⁹
Paranucler: A β_{40} and A β_{42}	Synthetic ^{19,28}

Table 1-1 Oligomer assemblies of A β and their origin.

1.1.6 Amyloid beta oligomer kinetics

The smallest oligomer sizes of A β , dimers and trimers, are very stable; they are not altered by SDS or 8 M urea^{23,24}. In contrast, the oligomerization process itself is very sensitive to denaturation conditions.

Chen and Glabe (2006) studied the oligomer kinetics of A β_{40} and A β_{42} *in vitro*. This study shows that A β_{42} oligomerization is time and concentration dependent. They incubated the two peptides at 50 μ M at room temperature in different concentrations of urea (Fig. 1-6). In 0.2 M urea oligomers begin to appear around 16-52 hours of incubation and increased with longer incubations (Fig 1-6). A β_{42} oligomerization is

concentration dependent, trimers and tetramers are formed at 25 μ M and 50 μ M but not at 12.5 μ M. A β ₄₀ did not assemble as trimers and tetramers. Urea concentrations >0.2 M already inhibited oligomer formation. Thus the appearance of oligomers requires native folded proteins to start with (a high enough concentration of urea can disrupt the native conformation of a protein)¹⁷.

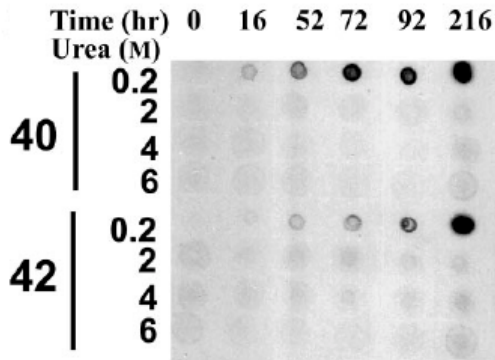


Figure 1-6 Oligomer formation kinetics. Samples at different time points were dotted on the nitrocellulose membrane. The membrane was probed by oligomer-specific antibody A11 without boiling. The spotted time is indicated above the blot and the urea concentration is indicated on the left side of the blot¹⁷.

1.1.7 Common fibril and oligomer structures of amyloids

The different amyloidogenic proteins found in amyloid deposits do not share apparent primary structure similarity. Although the oligomers and fibrils of the proteins are unrelated in primary sequence they do share similarity in their secondary structure, suggesting that the pathogenicity of amyloidogenic proteins is structure related and not sequence related².

The fibrils are long and unbranched and are composed of finer fibrils: the protofilaments. Amyloid fibrils can be ~10 nm in diameter and a micrometer in length, while the protofibrils are up to 150 nm in length and 5 nm in diameter (Fig. 1-5)²⁹. As stated above, amyloid fibrils have a common structural feature: the cross- β unit structure. X-ray fiber diffraction for different amyloid fibrils shows a cross- β diffraction pattern. There is a meridional reflection at ~4.7 Å and an equatorial reflection at ~10 Å (Fig. 1-7 A). This diffraction pattern is produced by the organization of specific parts of the peptides in the fibril as the cross- β structure³⁰.

The cross- β structure (Fig. 1-7 B) is composed of parallel, antiparallel or parallel and antiparallel β -sheets along the fibril axis. The intersheet spacing ranges from 5-14 Å. The β -strand segments in the β -sheets run perpendicular to the fibril axis by hydrogen-bonding up and down the sheet to identical molecules. The interstrand spacing is 4.7 Å. The structure and organization of the proteins in the fibrils is different for each amyloidogenic protein and have to be defined individually. Unfortunately fibrils have a noncrystalline insoluble nature thereby making structural studies very difficult³⁰.

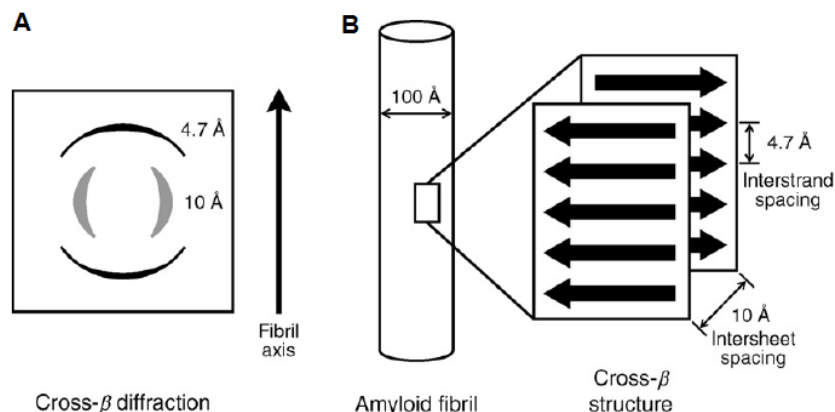


Figure 1-7 Cross- β structure of amyloid fibrils. (A) Drawing of the cross- β diffraction. (B) Cross- β structure of amyloid fibrils³⁰.

A common structural feature of the oligomer assemblies of amyloidogenic proteins is also suggested, since a study done by Kaye *et al.* (2003) was able to produce an oligomer-specific antibody that could recognize different amyloidogenic proteins. This suggests the presence of a shared structure in the different amyloidogenic proteins. In addition, this antibody can neutralize the pathogenicity of the oligomers *in vitro*, indicating a common pathological mechanism for all amyloidogenic proteins associated with this common conformation³¹.

1.1.8 Amyloid beta proposed structures

Conformation transition from α -helical to β -sheet

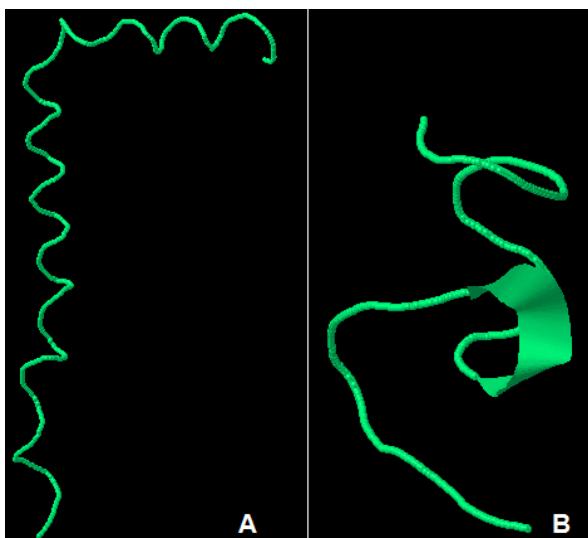


Figure 1-8 NMR structures of A β in different environments. (A) α -Helical structure of A β_{42} in apolar environment³². Image generated in Jmol from 1IYT. (B) Structure of A β_{10-35} in water as a collapsed coil²². Image generated in Jmol from 1HZ3.

A β aggregation is thought to be the result of a conformational transition from a mainly α -helical to a β -sheet conformation: the helix-coil-sheet progression¹⁵. The A β peptide *in vivo* is helical when it is part of APP and it has a β conformation in plaques¹⁶.

The conformation transition is hypothesized to be as followed: in the cell membrane when A β is part of APP, it has an α -helical conformation³². After cleavage and release in the extracellular space, the A β monomer forms a collapsed coil²² and starts to self-assemble into oligomers with still unknown conformations and sizes. The oligomers assemble further into protofibrils with β -sheet conformation and the protofibrils assemble into β -sheet fibrils¹⁹.

Amyloid beta monomer α -helical structures in apolar solution

There are many different studies that have studied solution structures (of different lengths) of A β peptides in apolar environment, such as mixtures of organic solvents with water and micellar solutions. The studies generally do not agree about the structure of A β in apolar solution, suggesting that the secondary structure of A β is strongly dependent on experimental conditions³². However the studies do agree that A β is mainly in an α -helical conformation in apolar environment (Fig. 1-8 A). This is consistent with the hypothesis that A β has an α -helical conformation in apolar environment *in vivo*; namely within the cell membrane¹⁶.

Amyloid beta monomer collapsed coil structure in polar solution

In water, A β adopts a collapsed coil that has no α -helical or β -sheet structure (Fig. 1-8 B). A β forms this conformation because it is more compact and has better solvation thermodynamics than the α -helical conformation²².

Amyloid beta fibril β -sheet structures

A β fibrils form β -sheet structure³³. A few fibril structure models of full-length A β peptides have been proposed so far.

A fibril model for A β ₁₋₄₀ based on solid state nuclear magnetic resonance (ssNMR) is proposed by Petkova *et al.* (2002). The ssNMR data suggests that residues 1-8 are disordered and they were omitted. The proposed structure consists of two β -strands (residues 9-24 and 30-40) separated with a bend formed by residues 25-29 (Fig. 1-9 A). The β -strands interact through side chain interactions. The side chains of residues D23 and K28 form a salt bridge. The β -strands form two in-register parallel β -sheets: the cross- β unit. The β -sheets run perpendicular to the fibril axis (Fig. 1-9 B). Two of these layers form a protofilament: the narrowest A β fibril. Two or more protofilaments pack together to form thicker fibrils (Fig. 1-9 C)³⁴.

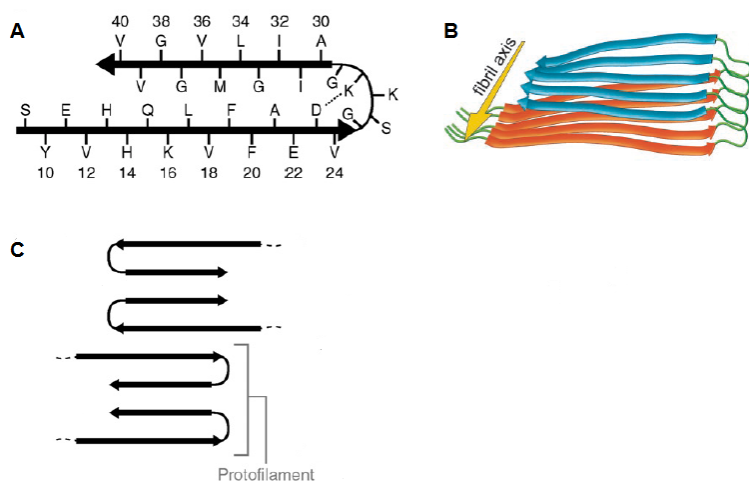


Figure 1-9 ssNMR model for A β ₁₋₄₀. (A) A β ₁₋₄₀ molecule, showing the two β -strands and bend³⁰. (B) The cross- β structure made of two in-register parallel β -sheets³⁴. (C) Lateral association of protofilaments to form thicker fibrils³⁰.

A comparable fibril model for A β ₁₋₄₂ has been proposed by Lührs *et al.* (2005). In this study they used quenched hydrogen-exchange NMR (qHX-NMR) on recombinant ³⁵Mox A β ₁₋₄₂. They suggest that residues 1-16 are disordered and that the two β -strands consist of residues 18-26 and 31-42 and the loop region of residues 27-30. The side chains of residues D23 and K29 form a salt bridge³⁵.

A slightly different model for A β ₄₀ using proline scanning mutagenesis has been proposed by Williams *et al.* (2004). Residues 1-14 and 37-40 are suggested to be disordered. Residues 15-21, 24-28 and 31-36 form β -strands (3 β -strands instead of two) and residues 22-23 and 29-30 form turns (Fig. 1-10)²⁰.

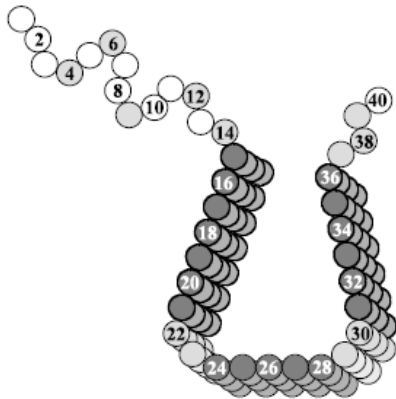


Figure 1-10 Proline scanning mutagenesis protofilament model for A β ₁₋₄₀. The 15-36 residues of the A β molecules are stacked in the direction parallel to the fibril axis²⁰.

1.1.9 Drugs against Alzheimer's disease

There are multiple possible targets to selectively inhibit the production, oligomerization or fibrillization of A β . It is important to determine which species are responsible for pathogenesis, because inhibiting fibrillization at a too late stage can cause accumulation of the pathogenic species and thereby accelerates the disease instead of preventing it⁷.

One could inhibit the liberation of A β from its precursor by inhibition of the secretases. This can be a dangerous approach with unwanted side effects. The secretases have enzymatic activities and process many important substrates. Thus a drug has to allow some activity of the secretases^{3,12}. Second, one could try to divert APP to follow the nonamyloidogenic processing pathway instead of the amyloidogenic pathway¹². Last, one could attempt to prevent oligomerization of A β with A β immunotherapy. Clinical trials with AD patients resulted in some promising results. Unfortunately some patients developed unwanted inflammatory reactions. One can also attempt to prevent oligomerization of A β with drugs that target the monomer and prevent oligomerization. The oligomers can also be targeted to prevent their pathogenicity³⁶.

There are a number of approaches that could be useful in AD therapies. Further characterization of the amyloid beta cascade is necessary to design safe and effective therapeutic drug therapies¹⁴.

1.2 Protein crystallography

The goal of protein crystallography is the production of a high-resolution molecular model to gain information about a protein its three-dimensional structure. The knowledge of a protein structure reveals insight into the protein its function. Interactions with other molecules can be studied, for example better understanding about how enzymes catalyze metabolic reactions, how they switch from an inactive to an active state by changing their conformation or how a protein binds to DNA, can be gained. With this information drugs targeting a specific part of the protein can be designed to inhibit unwanted protein functions. To obtain a molecular model using protein crystallography, the diffraction pattern of scattered X-rays caused by many highly ordered identical molecules in a protein crystal must be obtained and interpret. X-rays are used because their wavelength is small enough to be diffracted by the electron clouds surrounding a molecule. A crystal containing many ordered identically orientated protein molecules (which diffract identically) is necessary to produce strong enough diffracted X-ray beams that can be detected; the diffraction from a single molecule is too weak to be detected³⁷.

1.2.1 Crystallization

To be able to solve the structure of a protein, the protein must be expressed in large quantity and purified; a high-quality crystal must be obtained under optimal crystallization conditions. The protein solidifies into a crystalline state by the arrangement of the molecules in an ordered three-dimensional array (Fig. 1-11). A crystal is an array of many unit cells packed together to form a crystal; a unit cell is the smallest repeating element in a crystal. So knowing the content of one unit cell is like knowing the content of the whole crystal³⁷.

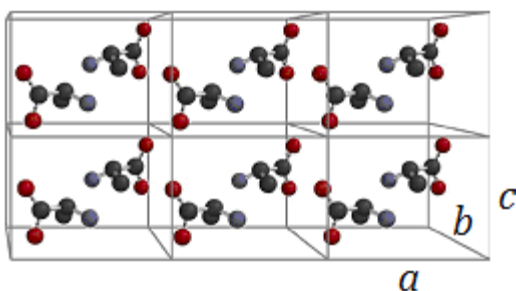


Figure 1-11 Six unit cells, each unit cell here consists of two alanine molecules. a , b and c are the edges of the unit cell³⁷.

The position of the atoms inside the unit cell is described by atomic positions measured from a lattice point (x_x, y_y, z_z) . These parameters make it possible to group crystal structures in crystal systems. For example crystals belonging to the orthorhombic crystal system have the lattice parameters: $a \neq b \neq c$, and α , β and γ are always 90° ⁴⁴.

Typical crystallization conditions contain buffer, precipitant and salt. Under favorable conditions a crystal will form, but most often precipitate or salt crystals will form or nothing happens at all. Successful crystallization is dependent on the salt, protein and precipitant concentrations, and pH and temperature. Finding the right condition takes a considerable trail and error and often many conditions must be tried before a condition that produces crystals is found, if any at all. Once a condition containing a good crystal is found, optimization of this condition (making small variations) is needed to produce high-quality crystals³⁷.

Crystals can form in a few days, several weeks or even months, it is therefore important

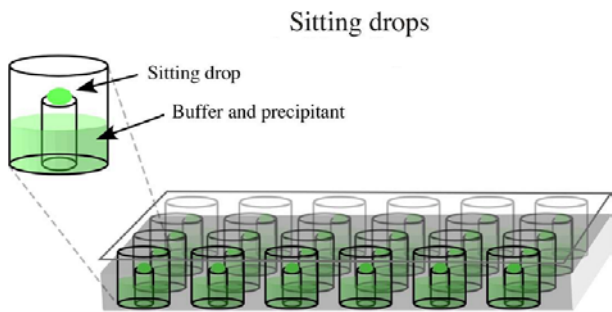


Figure 1-12 The sitting-drop method showing a well-plate, in which 24 sitting-drop crystallization trails can be carried out. Each well contains a pedestal with a concave top, in which the protein/crystallization drop sits. Vapor diffusion occurs between the drop and the reservoir containing buffer, precipitant and salt³⁷.

to continuously check the crystal plates for crystal formation. There are different crystallization methods including hanging-drop (in which the protein/crystallization solution drop hangs above a reservoir containing the crystallization solution) and sitting-drop methods (Fig. 1-12). There are crystallization robots available that can quickly set up systematically varied conditions. This is often used to get a quick impression of the crystallization conditions that promotes crystallization³⁷. In the mainly used vapor diffusion technique, equilibrium

between a protein/crystallization solution drop and a larger reservoir containing only crystallization solution is reached. Crystals are grown by slow precipitation from an aqueous solution. Water starts to evaporate slowly from the protein/crystallization solution drop to the reservoir until the precipitant concentration is the same in both solutions. The evaporation increases the protein and precipitant concentration, which promotes the first stage of crystal formation: nucleation. Nucleation is the formation of groups of molecules from which crystals start growing³⁷.

1.2.2 X-ray diffraction

Protein crystals are very fragile, that is because the molecules in the crystal are mainly held together by hydrogen bonds; non-covalent interactions. There are many different forms and sizes of crystals, all with different diffraction quality. Preferably only nicely formed crystals with sharp edges and smooth surfaces are screened on the X-ray machine for diffraction quality³⁷.

To prevent damaging the crystal by the X-ray beam, the crystal is kept flash frozen in a

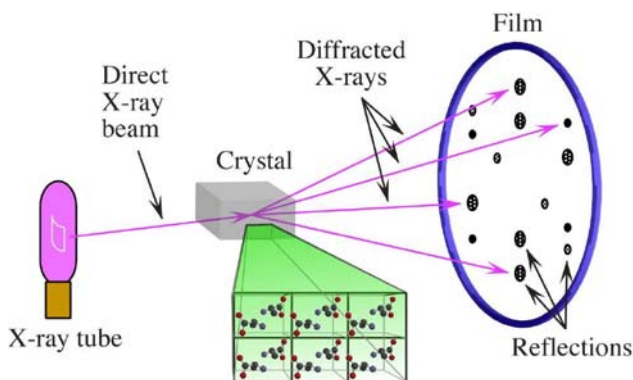


Figure 1-13 X-ray diffraction. The electron clouds in the crystal scatter the X-ray beam, producing diffracted X-rays each of which produces a spot (reflection) that can be detected³⁷.

liquid nitrogen stream. Freezing a crystal can also result in damage due to the formation of ice crystals, therefore the crystal is dipped in a cryoprotectant an ice-preventing agent. The crystal is removed from its mother liquor (the original crystallization solution) by picking it up in a circular loop of glass wool or synthetic fiber. Next the crystal is dipped in cryoprotectant and placed onto the goniometer of the X-ray source where it is kept in a constant stream of liquid nitrogen (120 K) to

flash-freeze it³⁷. When the X-ray beam strikes the crystal, the X-ray will be scattered by the electron clouds surrounding the molecules in the crystal and produce a diffraction pattern of spots known as reflections detected by an X-ray detector (Fig. 1-13). The diffraction pattern relates to atom positions in the molecules, while the intensity of each spot in the diffraction pattern correlates how strongly each atom diffracts in the molecule; this information is needed for solving protein structure along with known phase information. Depending on the crystal quality sharp spots should be visible and the crystal should diffract to at least 3 Å (Ångstrom) to be able to obtain an interpretable electron-density map. If that is the case, collecting a full data set can be considered³⁷.

1.2.3 The phase problem

To be able to calculate the electron density based on the diffraction pattern three parameters of each reflection must be measured: the amplitude, frequency and phase. The amplitude and frequency are accessible in the data that is obtained, while the phase is not. The phase angle for each reflection has to be determined. It can be determined with three different techniques: isomorphous replacement, anomalous scattering or molecular replacement³⁷.

In the isomorphous replacement approach, a heavy atom is added, thereby changing the diffraction pattern compared to the diffraction pattern of the native crystal. The change in diffraction pattern can be used to obtain estimates of the phase angle³⁷.

Anomalous scattering is also based on adding a heavy atom. Heavy atoms have an absorption edge near the wavelength of X-rays³⁷. Collection of three data sets from the same crystal at different wavelength around the absorption edge of the anomalous scatterer makes it possible to determine the phase⁴⁵.

Molecular replacement makes use of a phasing model to determine the structure of the new protein. The phasing model is a known homologous protein with at least 25% sequence identity. The phases can be calculated by placing the model of the known protein in the unit cell of the new protein³⁷.

1.2.4 Model building

Once an electron-density map is obtained a molecular model can be built into the density. The model must be in agreement with the principles of molecular structure and stereochemistry and must fit into the electron density³⁷. To improve the model it can be refined against the data to improve the phases, which results in a clearer map and a clearer model. This is done to make the model in better agreement with the data. This cycle is repeated several times until no further improvement is made and hopefully an accurate model results^{37,45}. Occasionally portions of the known sequence of a protein cannot be found back in the electron-density map. That can be because the region is disordered or flexible. It is also not uncommon for termini residues to be missing from the model³⁷.

1.3 Aim and procedure

More and more evidence indicates that especially the soluble A β oligomers are neurotoxic and play an important role in the Alzheimer's disease related pathology^{4,5,23,25}. Therefore the ultimate aim of this study is to solve the structure of human A β ₄₂ in an oligomeric state for rational structure based drug design against Alzheimer's disease.

Protein purification and X-ray crystallography techniques are being used. Due to the extreme insolubility of A β it is hard to separate and thereby purify it from the other proteins in solution. All the crystallography structures proposed so far are fragment peptides of A β ³⁸ (Sup. 1).

To be able to study A β with X-ray crystallography, A β was previously linked to the full-length chaperonin protein GroEL at the last residue of GroEL residue D523 (Fig. 1-14) (see Sup. 2 for background information of GroEL). It is difficult to trap A β in an oligomeric state because of its hydrophobic nature and high propensity for aggregation. Protecting A β inside the tunnel of GroEL will limit its oligomerization and thus its aggregation. GroEL forms a heptamer with an internal cavity in which A β was situated. In this manner, A β was prevented from self-association into insoluble fibrils; it can only form oligomeric states up to heptamers. Unfortunately, this specific protein complex assembly has not resulted in the structure of A β yet.



Figure 1-14 Center view of the full-length GroEL monomer. A β ₄₂ was linked to residue D523. Image generated in SPOCK from the structure with Protein Data Bank identification (PDB ID) code: 1GRL.

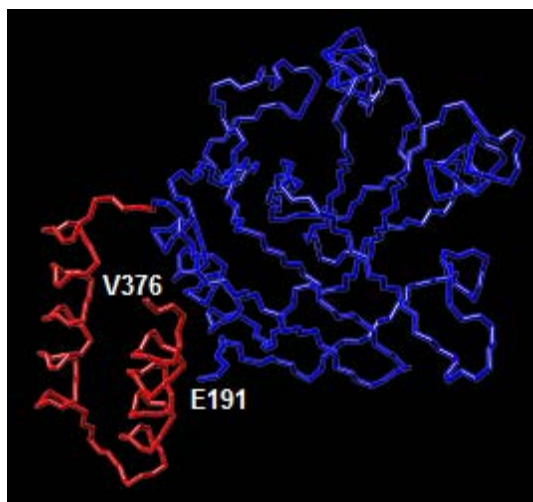


Figure 1-15 Apical domain of GroEL. In blue apical residues E191-V336. In red the last two helices of the apical domain, residues G337-V376. Image generated in Chimera from PDB ID code: 1KID.

In this study A β is linked to the apical domain of GroEL (residues 191-376 of GroEL) (Fig. 1-15), creating the fusion protein ApicalGroEL-A β . In the fusion protein, A β is fused to the C-terminal end of the apical domain of GroEL (residue V376). This approach should allow for more flexibility, as A β is no longer trapped in a tunnel. At the same time, it inhibits the fibrillization and prevents A β precipitation, thereby forming the

possibility to trap A β as an oligomer. The apical domain of GroEL does not have the propensity to oligomerize; therefore any oligomer formation is thought to be A β dependent.

Multiple ApicalGroEL-A β fusion protein constructs are built, with a general construction (Fig 1-16). They contain a N-terminal His-tag followed by the apical domain of GroEL. In between the apical domain and A β a synthetic sequence, the so-called linker is placed. The constructs vary in the following three characteristics.

Different linkers are placed in between GroEL and A β to manipulate the arrangement of A β . The tested linkers are distinguished from each other by their length and hydrophobicity. Also, different size combinations of the apical domain of GroEL and A β are tested. Regarding the apical domain of GroEL constructs with and without residues 337-376 are tested; A₁₉₁₋₃₇₆ and A₁₉₁₋₃₃₆. A₁₉₁₋₃₃₆ does not contain the last two helices that are present in A₁₉₁₋₃₇₆ (Fig. 1-15). This is done to manipulate the packing of GroEL and A β in the unit cell. It is known that the first 16 residues of A β are disordered¹⁶. Therefore, in this study constructs with and without residues 1-16 are tested; A β ₁₋₄₂ and A β ₁₇₋₄₂.

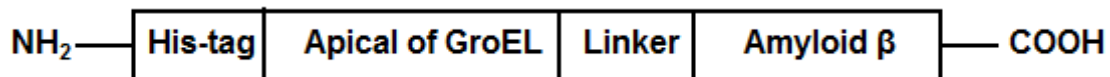


Figure 1-16 The fusion protein ApicalGroEL-A β .

In summary, different combinations of apical GroEL, linkers and A β are built, the ApicalGroEL-A β constructs are expressed and purified and the monomer and different oligomeric states present are also separated for crystallization purposes. All together these constructs are made with the hopeful expectation that one or more of them result in the formation a conformation of A β linked to GroEL as an oligomer that produces well diffracting crystals.

Two different crystallization approaches are used. The first approach is to isolate the protein as a monomer and screen for crystallization. Since A β has the propensity to form oligomers when it is at a high enough concentration¹⁷, the assumption is made that the protein will oligomerize as a result of concentration and crystallize as an oligomer. The second approach is to isolate ApicalGroEL-A β in an oligomeric state and to crystallize the protein in this oligomeric state. The protein monomer is purified, brought to high concentration and incubated to see if it will form oligomers in a time dependent manner, which can be purified and crystallized.

On our way to well diffracting crystals the following questions are tried to be answered:

- Do the constructs that vary in the size of the apical domain, linker length and hydrophobicity, and A β truncation show specific properties compared to each other?
- In what state(s) (monomeric and/or oligomeric) is it possible to purify and crystallize the protein?
- Is the monomer that is observed composed of the whole ApicalGroEL-A β protein or is it being cleaved?
- Is A β still present in the crystals or is A β cleaved off and are the crystals made of cleaved ApicalGroEL-A β protein?

- Is it possible to assemble the protein to an oligomeric state in a time-dependent manner?
- What are the approximate sizes of the oligomers that are observed?
- Are the observed oligomers composed of the whole protein or are the oligomers formed of cleaved protein?
- Which ApicalGroEL-A β protein construct(s) is/are best to use for our aim?
- Are there ApicalGroEL-A β protein constructs as a monomer or as an oligomeric state that produce well diffracting crystals?

Different techniques are used to answer these questions. Purification techniques such as affinity and size exclusion chromatography are used to purify the different protein assemblies. Sitting drop methods are used to crystallize ApicalGroEL-A β . For molecular weight analysis, size exclusion chromatography and mass spectrometry are used. Dynamic light scattering is used to monitor oligomer formation and western blots are used to analyze the composition of the protein.

Eventually the most crucial question has to be answered:

Is it possible by solving the structure of A β in an oligomeric state to gain better understanding of the A β mechanism in order to design drugs against Alzheimer's disease?

Chapter 2; Materials and methods

2.1 General experiments: plasmid, gene and protein constructs

The ApicalGroEL-A β constructs that were built had a general construction (Fig. 1-16 and 2-1). The constructs had a N-terminal polyhistidine-tag (6X-His-tag) that has affinity for nickel ions that can be used for affinity purification. Followed by the apical domain of GroEL, the linker region and most C-terminal A β . The amino acid sequences and molecular weights of the built constructs can be found in supplement 8. The vector that was used to insert and express the genes of interest in is pET-28b [Novagen]. The linkers were ordered directly from Integrated DNA Technologies. The linker nucleotide sequences can be found in supplement 7. The sequence of the apical domain of GroEL was in a previous study amplified from the *E.coli* genome (strain K12). A β_{1-42} was in a previous study amplified from human brain cDNA. The ApicalGroEL-A β constructs listed in table 2-1 were built using the molecular cloning techniques as described in the next section.

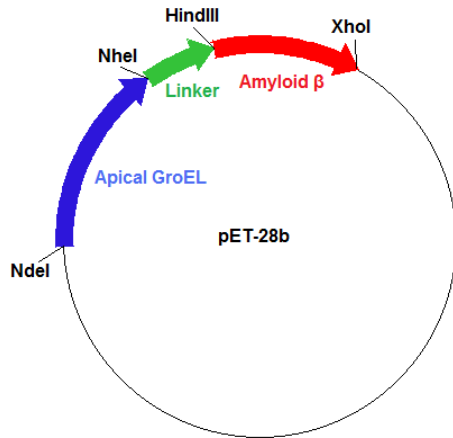


Figure 2-1 ApicalGroEL-A β gene construction, also showing four specific restriction sites.

Construct name	GroEL residues	Linker (amino acid sequence)	A β residues
A376-SAG-A β 42	Apical 191-376	SAG	A β 1-42
A376-6SAG-A β 42	Apical 191-376	SAGSAG	A β 1-42
A376-9SAG-A β 42	Apical 191-376	SAGSAGSAG	A β 1-42
A376-12SAG-A β 42	Apical 191-376	SAGSAGSAGSAG	A β 1-42
A376-6MPT-A β 42	Apical 191-376	MPTATA	A β 1-42
A376-9NSQ-A β 42	Apical 191-376	NSQPNTNGS	A β 1-42
A376-12NSS-A β 42	Apical 191-376	NSSGSGSNSSGS	A β 1-42
A376-6SAG-A β 17-42	Apical 191-376	SAGSAG	A β 17-42
A336-6SAG-A β 42	Apical 191-336	SAGSAG	A β 1-42
A336-12GSA-A β 42	Apical 191-336	GSAGSAAGSGEF	A β 1-42
A336-6SAG-A β 17-42	Apical 191-336	SAGSAG	A β 17-42
A376 control	Apical 191-376		
A336 control	Apical 191-336		

Table 2-1 ApicalGroEL-A β constructs.

2.2 General experiments: cloning of the ApicalGroEL-A β constructs

2.2.1 Plasmid preparation

Double digestion

To digest 1 μ g (see section 2.8.4 for DNA concentration measurement) of plasmid pET-28b, 5 μ l (10x) Buffer 2 [New England Biolabs] and 20 Units (U) of both of the appropriate restriction enzymes [New England Biolabs] were added to 1 μ g plasmid. MilliQ water (mQ) was added to get an end volume of 50 μ l. The chosen restriction enzymes were depending on which gene/linker had to be inserted (Fig. 2-1 and Tab. 2-2). The reaction mixture was incubated at 37 °C for 3 hours. The DNA was separated by size with an agarose gel (see section 2.8.1 for DNA separation by agarose gel).

Gene or linker to insert in pET28b	Restriction enzyme 1	Restriction enzyme 2	Forward primer	Reverse primer
Apical 191-376	NdeI	NheI	NdeI apical	Apical 376 NheI
Apical 191-336	NdeI	NheI	NdeI apical	Apical 336 NheI
Apical 191-376 control	NdeI	XhoI	NdeI apical	Apical 376 XhoI
Apical 191-336 control	NdeI	XhoI	NdeI apical	Apical 336 XhoI
SAG	NheI	HindIII	NheI SAG	A β XhoI
SAGSAG	NheI	HindIII	NheI SAGSAG	A β XhoI
SAGSAGSAG	NheI	HindIII	NheI SAGSAGSAG	A β XhoI
SAGSAGSAGSAG	NheI	HindIII	NheI SAGSAGSAGSAG	A β XhoI
MPTATA	NheI	HindIII	NheI MPTATA	A β XhoI
NSQPNTNGS	NheI	HindIII	NheI NSQPNTNGS	A β XhoI
NSSGSGSNSSGS	NheI	HindIII	NheI NSSGSGSNSSGS	A β XhoI
GSAGSAAGSGEF	NheI	HindIII	NheI GSAGSAAGSGEF	A β XhoI
A β 1-42	HindIII	XhoI	HindIII A β 1-42	A β XhoI
A β 17-42	HindIII	XhoI	HindIII A β 17-42	A β XhoI

Table 2-2 Genes and linkers respective restriction enzymes and primers.

DNA extraction from agarose gel

The DNA was visualized under UV light and the double digested plasmid DNA band was cut out and the weight of the gel slice was measured. The DNA was extracted using the QIAquick Gel Extraction Kit [Qiagen] as followed.

Three volumes of Buffer QG were added to one gel volume (100 mg for 100 μ l) and this was incubated in a heating block at 50 °C for 10 min until the gel slice was completely dissolved. To help dissolving the gel, the tube was vortexed every few minutes. Next one gel volume of isopropanol was added and mixed carefully. The solution then was applied to a Qiaquick spin column with collection tube and centrifuged for one minute at 13,200 rpm. The flow-through was discarded and applying 750 μ l of buffer PE to the column and centrifuging for another minute washed the column. After discarding the flow-through the column was again centrifuged to make sure that all residual ethanol from Buffer PE was removed. Next the spin column was placed in an eppendorf tube and for elution of the DNA 30 μ l mQ was directly applied to the center of the column membrane, incubated for five minutes and centrifuged for one minute. To remove all traces of ethanol the purified DNA was speedvaced for 10 minutes. The sample was now ready for ligation and could be used immediately or stored at -80 °C for later use.

2.2.2 Insert preparation

Linker preparation

The designed oligonucleotides were ordered from Integrated DNA Technologies, one of them included a 5' partial NheI restriction site while the other one had a 5' partial HindIII

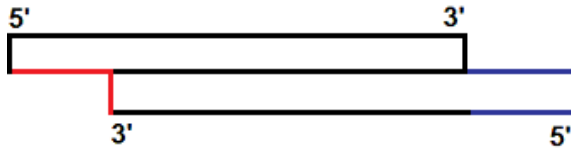


Figure 2-2 Linker construct. Two oligonucleotides annealed to each other. The red overhang contains a partial NheI restriction sequence. The blue overhang contains a partial HindIII restriction sequence.

restriction site (Fig. 2-2). The forward and reverse oligonucleotides were both diluted to 100 μ M with mQ to a final volume of 100 μ l. These solutions were mixed together and vortexed to get a 200 μ l duplex solution (100 μ M). This was split into two PCR tubes and the following thermocycler annealing protocol was started:

94 °C	T _m + 10 °C	T _m + 5 °C	T _m - 2 °C	T _m - 7 °C	T _m - 12 °C	T _m - 20 °C	4 °C
2 min	5 min	5 min	2 min	2 min	2 min	10 min	∞

After finishing the reaction the linker duplex was ready for ligation and could be used immediately or stored at -80 °C for later use.

Gene preparation

The inserts were made by amplifying from plasmid constructs containing the gene of apical domain of GroEL and the gene of A β ₄₂. These inserts were: apical 191-376, apical 191-336, A β 1-42 and A β 17-42. See supplement 6 for primer nucleotide sequences and additional information.

PCR amplification

The designed primers were ordered from Integrated DNA Technologies. The primers were brought into solution by adding 1 μ l mQ per nM primer making it a 1mM primer solution. This was diluted further to a 10 μ M primer solution by adding 2 μ l of 1 mM primer solution to 198 μ l mQ.

A 300 μ l PCR reaction mixture was prepared containing 6 μ l (10 μ M) of both of the appropriate forward and reverse primers (Tab. 2-2), 6 μ l plasmid construct containing the desired gene and 282 μ l PCR SuperMix High Fidelity [Invitrogen]. This was split into 50 μ l reactions in PCR tubes and the following PCR protocol was started:

	25x					
94 °C	94 °C	54 °C	69 °C	68 °C	4 °C	
2 min	30 sec	30 sec	45 sec	7 min	∞	

After finishing the reaction a few microliters were taken and ran on an agarose gel to confirm specific amplification. After confirmation the sample was ready for a PCR product purification to remove the primers and enzyme and could be used immediately or stored at -80 °C for later use.

PCR product purification

To remove the primers and enzyme three volumes of Buffer PB [Qiagen] were added to one volume of PCR reaction mixture, this was carefully mixed and applied to a Qiaquick spin column [Qiagen] with collection tube. This was centrifuged for one minute at 13,200 rpm and the flow-through was discarded. Applying 700 μ l of Buffer PE [Qiagen], incubating it for a few minutes and centrifuging for another minute washed the column. After discarding the flow-through the column was centrifuged for 5 minutes to make sure that all residual ethanol from Buffer PE was removed. Next the QIAprep spin column was placed in an eppendorf tube and for eluting the DNA 100 μ l mQ was directly applied to the center of the column membrane incubated for five minutes and centrifuged for one minute. Next another 50 μ l of mQ was applied to the membrane, incubated and centrifuged. To remove all traces of ethanol the purified DNA was speedvaced for 10 minutes. The sample was now ready for further use and could be used immediately or stored at -80 °C for later use.

Double digestion

The digestion protocol for the inserts is the same as is used for plasmid digestions, digesting 1 μ g in a 50 μ l reaction volume (see section 2.2.1).

Digested PCR product purification

The purification after digestion is the same as the PCR product purification protocol except for the elution step. The DNA was eluted first with 30 μ l mQ and next with another 20 μ l more mQ. The sample was now ready for ligation and could be used immediately or stored at -80 °C for later use.

2.2.3 Ligation and transformation

Linker ligation into cut plasmid

10 μ l of linker (100 μ M) and 5 μ l of the double digested plasmid with NheI and HindIII were added together and mixed slightly. Of the DNA Dilution Buffer [Roche Applied Science] 2.5 μ l was added to the tube. Next 10 μ l of DNA Ligation Buffer [Roche Applied Science] was also added to the tube. Finally 2 μ l of T4 DNA Ligase [Roche Applied Science] was added, the reaction was mixed carefully and the reaction was incubated at room temperature for 10 minutes. The ligation reaction was now ready for the transformation.

Gene ligation into cut plasmid

A slightly different protocol was used to ligate the bigger inserts apical 191-376, apical 191-336, A β 1-42 or A β 17-42 into the double digested plasmid (digested with the correct enzymes depending on which insert had to be inserted (Tab 2-2)).

A molar ratio of vector DNA to insert DNA of 1:5 was used. Of the plasmid 100 ng was used for the reaction. Depending on the molar ratio and size of the plasmid and the insert, the required amount of insert DNA was calculated (in ng). After adding the right amount of plasmid and insert DNA together, 2 μ l of DNA Dilution Buffer was added and mQ water was added to get an end volume of 10 μ l. In a separate tube 11 μ l DNA Ligation Buffer was mixed carefully with 1 μ l T4 Ligase until the solution was homogenous. This

was then added to the DNA/buffer solution and again mixed carefully. The reaction was incubated at 25 °C for 10 minutes in a thermocycler. The ligation reaction was now ready for the transformation.

Plasmid transformation into NovaBlue competent cells

An eppendorf tube containing 50 µl NovaBlue Singles™ Competent Cells [Novagen] (*E.coli*) was thawed on ice. Next 5 µl ligation reaction was added carefully to the competent cells. The ligation reaction with the competent cells was incubated for 30 minutes on ice, followed by a heat shock in a 42 °C water bath for 30 seconds. After this the cells were put back on ice immediately for 2-5 minutes and 150 µl of SOC medium [Novagen] was added to rescue the cells. This was incubated in a 37 °C shaker for one hour and 60 µl was plated on a Luria-Bertani (LB) agar plate containing the antibiotic kanamycin (see section 2.8.7 for LB agar plate preparation). The plate was incubated overnight in a 37 °C incubator.

2.2.4 ApicalGroEL-Aβ construct confirmation

Overnight cultures

After a successful ligation and transformation, bacteria colonies were present on the LB agar plate. To be able to confirm the insertion of the desired gene/linker into the plasmid a small 10 ml LB culture (see section 2.8.8 for LB culture preparation), with added kanamycin antibiotic (100 µg/ml final concentration) was inoculated with a bacterial colony and this was grown overnight in a 37 °C shaker.

Plasmid isolation

The plasmid was isolated using the QIAprep Spin Miniprep Kit [Qiagen]. The overnight culture was centrifuged for at least 10 minutes at 3,000 rpm to collect the cells. The supernatant was discarded and the pellet was resuspended in 250 µl Buffer P1 and transferred to an eppendorf tube. Next 250 µl of Buffer P2 was added and inverting the tube 4-6 times mixed this. Of Buffer N3 350 µl was added and this was mixed immediately by inverting the tube 4-6 times. This was centrifuged for 13 minutes at 13,200 rpm. The supernatant was applied to the QIAprep spin column with collection tube, this was centrifuged for one minute at 13,200 rpm and the flow-through was discarded. Applying 750 µl of Buffer PE and centrifuging for another minute washed the column. After discarding the flow-through the column was centrifuged for 5 minutes to make sure all residual ethanol from Buffer PE was removed. Next the QIAprep spin column was placed in an eppendorf tube and for eluting the DNA 60 µl mQ was applied to the center of the column membrane incubated for five minutes and centrifuged for one minute. To remove all traces of ethanol the purified DNA was speedvaced for 10 minutes. The sample was now ready for further use and could be used immediately or stored at -80 °C for later use.

PCR to confirm construct

To confirm the insertion of the gene/linker into the plasmid a PCR was performed on the plasmid DNA with insert specific primers. For both of the appropriate forward and reverse primer 0.25 µl (10 µM) was applied to a PCR tube with 0.25 µl plasmid and 11.75

μl PCR SuperMix High Fidelity [Invitrogen]. The following PCR protocol was started:

	25x					
94 °C	94 °C	54 °C	69 °C	68 °C	4 °C	
2 min	30 sec	30 sec	45 sec	7 min	∞	

After finishing the reaction, the mixture was loaded and run on an agarose gel. A clear band of the correct size confirmed insertion of the gene.

Sequencing to confirm construct

To check the DNA sequence of the built construct 500 ng of plasmid DNA was sent to the Gene Technology Laboratory, Institute of Developmental and Molecular Biology at Texas A&M University.

2.3 General experiments: expression of the ApicalGroEL-Aβ constructs

An expression test was done to check if the cells were able to express ApicalGroEL-Aβ and to see if ApicalGroEL-Aβ was in the soluble fraction.

2.3.1 Plasmid transformation into BL21 competent cells

The plasmid construct was transformed into the expression strain BL21(DE3) Singles™ Competent Cells (*E.coli*) [Novagen] and 2 μl plasmid was added to the competent cells. This was incubated on ice for 30 minutes, followed by a heat shock in a 42 °C water bath for 30 seconds. After this the cells were put back on ice immediately for 2-5 minutes and 150 μl of SOC medium [Novagen] was added to rescue the cells. This was incubated in a 37 °C shaker for one hour and 20 μl was plated on a LB agar plate containing the antibiotic kanamycin. The plate was incubated overnight in a 37 °C incubator.

2.3.2 Expression test

After a successful transformation, bacteria colonies were present on the LB agar plate. A 10 ml LB culture, with added kanamycin antibiotic (100 μg/ml final concentration) was inoculated with a bacterial colony and this was incubated overnight in a 37 °C shaker. Next day the culture was diluted in a new 10 ml LB culture (containing 100 μg/ml final concentration kanamycin) so it would reach an optical density (O.D.) of about 0.8-1.0 (see section 2.8.6 for bacterial growth measurement).

For a 37 °C expression test, the cells were induced with isopropyl-β-thiogalactopyranoside (IPTG: 1 mM final concentration) to start the protein expression. The undiluted cells that were not induced with IPTG served as a control. The tubes were placed in a 37 °C shaker for three hours. After this the cells were ready for lysis (see below).

For an 18 °C expression test, the cells were also diluted to an O.D. of about 0.8-1.0 and cooled down on ice to 18 °C before inducing with IPTG. The undiluted cells that were not induced with IPTG served as a control. The tubes were placed in an 18 °C shaker for at

least 18 hours, after this the cells were ready for lysis.

To be able to lyse the cells, the cells were spun down for 10 minutes at 3,000 rpm. The supernatant was discarded and the cells were resuspended in 150 μ l lysis solution (lysis solution: 1 ml BugBuster® Master Mix [Novagen] and 30 μ l DNase (20 mg/ml).

10 μ l was taken to load on a SDS-PAGE gel as lysate fraction. The cells were put on ice for 5 minutes and spun down for 3 minutes at 3,200 rpm. Of the supernatant 10 μ l was taken to load on the SDS-PAGE gel too. Next, these samples were loaded on a SDS-PAGE gel (see section 2.8.2 for protein separation by SDS-PAGE).

2.4 General experiments: ApicalGroEL-A β purification

2.4.1 Cell growth and protein production

A starter culture, 1 L LB media (see section 2.8.9 for LB media preparation) containing kanamycin (100 μ g/ml final concentration) was inoculated with a colony of a LB agar plate with the *E.coli* strain BL21 containing one of the plasmid constructs. This was incubated overnight in a 37 °C shaker. Next day the culture was diluted in a two 1.5 L LB media (containing 100 μ g/ml final concentration kanamycin) so they would reach an O.D. of about 0.8. The 1.5 L LB media containing flasks were put on ice for about 20 minutes to cool them down to 18 °C. Next it was induced with IPTG (1 mM final concentration) and incubated in an 18 °C shaker for at least 18 hours.

2.4.2 Cell lysis

The cells were spun down in 1 L centrifuge bottles for 40 minutes at 4,000 rpm at 4 °C, next the supernatant was discarded and the pellets were resuspended in 7 ml Ni²⁺ column buffer A (20 mM Tris, 300 mM NaCl and 20 mM imidazole, pH 7.5). To each 50 ml of resuspended cells 100 μ l DNase (20 mg/ml), 100 μ l phenylmethanesulfonyl fluoride (PMSF: 0.1 M) and 1 ml protease inhibitor cocktail Set V EDTA-Free [Calbiochem] were added. The cells were lysed mechanically with a French Press. French Press uses high pressure to lyse the cells by forcing the cells through a small hole in the press. For each 50 ml of cells two rounds were performed to lyse the cells efficiently. A small amount of sample was saved to run on a SDS-PAGE as lysate. Next the cells were spun down in 50 ml centrifuge tubes for 40 minutes at 15,000 rpm at 4 °C. Some pellet was saved to run on the SDS-PAGE. The supernatant was filtered using a syringe [BD] with 0.45 μ m syringe filter [Pall corporation]. Some supernatant was also saved to run on the SDS-PAGE. The supernatant was now ready for purification.

2.4.3 Nickel affinity chromatography

The N-terminal His-tag of the ApicalGroEL-A β constructs with affinity for nickel ions made purification possible using a Ni²⁺ column. The fast protein liquid chromatography (FPLC) pumps were washed with an excess of filtered mQ to clean the pumps. Next a Ni²⁺ column [GE Healthcare] was connected to the pumps and it was washed with 10 column volumes of Ni²⁺ column buffer B (20 mM Tris, 300 mM NaCl and 500 mM

imidazole, pH 7.5) to remove all the proteins from the column. Followed by equilibration with 10 column volumes of Ni²⁺ column buffer A (20 mM Tris, 300 mM NaCl and 20 mM imidazole, pH 7.5). The protein solution was loaded onto the column and a wash with buffer A removed all unbound proteins. The flow-through was collected to run as a sample on a SDS-PAGE. An elution protocol was started, collecting 90 2.2 ml fractions with a fraction collector [Pharmacia Biotech]. During the protocol the concentration of buffer B was increased linearly till a final concentration of 70% over 200 ml, the high concentration of imidazole in buffer B competed with and released the His-tag bound protein from the Ni²⁺ column. A SDS-PAGE was run to check the presence of pure protein in the different fractions.

2.5 ApicalGroEL-A β isolation as a monomer

In this approach the ApicalGroEL-A β monomer was isolated and screened for crystallization. Since A β has the propensity to form oligomers when it is at a high enough concentration¹⁷ (section 1.1.6), the assumption was made that the protein would oligomerize as a result of concentration and crystallize as an oligomer. Additional experiments were performed to analyze if the ApicalGroEL-A β protein was crystallized and not a cleavage product.

2.5.1 Crystallization preparation

After nickel column purification (see section 2.4.3 for nickel affinity chromatography) the fractions containing the most pure ApicalGroEL-A β monomer bands on SDS-PAGE were pooled. The protein pool was split and put in two Spectra/Por® Dialysis Membrane dialysis bags (12-14 kDa) [Spectrum Laboratories, Inc.]. One bag was put in dialysis buffer containing no glycerol (20 mM Tris and 100 mM NaCl, pH 7.5) and one in dialysis buffer with glycerol (20 mM Tris, 100 mM NaCl and 5% glycerol, pH 7.5). This was set overnight at 4 °C to remove the imidazole and high salt concentration. Next day the protein was concentrated to the desired concentration using an Amicon Ultra-15 Centrifugal Filter (10 kDa) [Millipore] by centrifuging at 3,000 rpm (see section 2.8.5 for protein concentration measurement). The ApicalGroEL-A β protein was now ready for crystallization screening or optimization.

2.5.2 Crystallization screening

After concentrating ApicalGroEL-A β to the desired concentration it was transferred to an eppendorf tube and spun down at 13,200 rpm at 4 °C for twenty minutes to remove any precipitation. To automatically set up systematically varied crystallization conditions, a hydra microdispenser was used [Robins Scientific corporation]. The protein, an Intelli-plate 96 well [Hampton Research] and 96 well screen containing 96 different crystallization solutions (Crystal Screen 1&2 [Hampton Research], Wizard Screen 1&2 [Emerald BioSystems], or PEG/ION 1&2 [Hampton Research]) were placed on the pipetting station of the robot. A protocol was started that dispensed drops in the 96 well Intelli-plate. In the reservoir, crystallization solution was dispensed and on the pedestals different ratios of ApicalGroEL-A β and crystallization solution were dispensed; buffer to

protein 2:1 and 1:1. The Intelli-plate was sealed with a ClearSeal Film[™] [Hampton Research] and the crystallization screen was sealed with AlumaSeal II Film [Phenix research]. The Intelli-plate was placed in the crystallization room at 16 °C.

2.5.3 Crystallization optimization

After concentrating ApicalGroEL-A β to the desired concentration it was transferred to an eppendorf tube and spun down at 13,200 rpm at 4 °C for twenty minutes to remove any precipitation. A 72 well Microbatch plate [Greiner] was filled with 5 ml of oil. Different crystallization solutions self-made, or pre-made ordered from Hampton Research were added into the drop well. Next ApicalGroEL-A β was added to the drop well. Different buffer to protein ratios were used. The Microbatch plate was placed in the crystallization room at 16 °C.

2.5.4 Structure determination and refinement

Diffraction data from a crystal flash-frozen in liquid nitrogen at 120 K was collected using the R-Axis IV image plate detector in the laboratory or data was collected at the Advanced Proton Source (Argonne National Laboratory, Chicago) at beamline 23ID. The data was processed with HKL-2000. Structures were determined by molecular replacement using the phases from the determined crystal structure of the apical domain of GroEL (PDB ID code: 1KID) using the program CCP4. Model rebuilding was performed with Coot and the structure was refined using Phenix.

2.5.5 Monomer cleavage analysis

The smaller molecular weight bands of ~10-20 kDa that were observed on SDS-PAGEs (Fig. 3-3) of nickel column purifications are suggested to be cleavage products of ApicalGroEL-A β . To analyze the observed cleavages mass spectrometry and western blot analysis was used.

Mass spectrometry

Mass spectrometry is a technique that can determine the mass-to-charge ratio of the (charged) molecules in a sample. Based on the mass-to-charge ratio the masses of the sample components can be derived.

For mass spectrometry analysis the fractions containing the most pure monomer of construct A336-6SAG-A β 42 after nickel column purification were pooled. The protein was concentrated to 15 mg/ml using an Amicon Ultra-15 Centrifugal Filter (10 kDa) [Millipore] by centrifuging at 3,000 rpm. The Protein Chemistry Laboratory, Department of Biochemistry & Biophysics at Texas A&M University analyzed the sample with a time of flight mass spectrometer; an Axima-CFR instrument [Kratos analytical].

2.5.6 Crystal composition analysis

To analyse the composition of the protein crystals, dissolved crystals were analyzed with western blotting.

Crystals of ApicalGroEL-A β construct A376-6SAG-A β 42 from a microbatch plate containing crystallization solution Wizard screen I condition 31 were picked up with a loop and washed a few times in 10 μ l dialysis buffer (20 mM Tris, 100 mM NaCl and 5% glycerol, pH 7.5) to remove the well solution and any oil that was possibly stuck on the crystal surface. Next the crystals were dissolved in 15 μ l dialysis buffer thoroughly. The crystals were loaded on a SDS-PAGE following the western blot protocol (see section 2.8.3 for western blot analysis).

2.6 ApicalGroEL-A β isolation as an oligomer

2.6.1 Time dependent oligomerization analysis

In this approach it was tried to isolate and crystallize ApicalGroEL-A β in an oligomeric state. The protein monomer was isolated, brought to high concentration to see if it would form oligomers in a time dependent manner that could be isolated and crystallized. This approach is inspired by the fact that A β oligomerization is known to be concentration and time dependent¹⁷ (section 1.1.6). The ApicalGroEL-A β monomer after nickel column purification was further purified with a gel filtration column, a SuperdexTM 75. After bringing to high concentration the protein was incubated at room temperature. Aliquots at different time points of incubation were analyzed with dynamic light scattering and western blotting to monitor the time dependent oligomerization.

Superdex 75 size exclusion chromatography

After nickel column purification the fractions containing the most pure protein monomer bands on SDS-PAGE of construct A336-6SAG-A β 42 were pooled.

The SuperdexTM 75 (S75) column [GE Healthcare] has a separation range for globular proteins of 3 kDa - 70 kDa. The FPLC pumps were washed with an excess of filtered mQ to clean the pumps. Next the column was connected to the pumps and equilibrated overnight with at least 5 column volumes of S75 buffer (20 mM Tris and 100 mM NaCl, pH 7.5). The nickel column purified monomer pool was concentrated down to 1 ml and loaded onto the S75 column with a syringe [BD]. An elution protocol was started collecting 90 2.2 ml fractions over 200 ml with a fraction collector [Pharmacia Biotech]. A SDS-PAGE was run to find the fractions containing the protein monomer and these fractions were pooled.

Room temperature incubation

The fractions containing the most abundant and pure monomer (based on SDS-PAGE analysis) were concentrated down to 30.40 mg/ml using an Amicon Ultra-15 Centrifugal Filter (10 kDa) [Millipore] by centrifuging at 3,000 rpm.

One fraction was threaded separately, fraction 42 because that fraction was observed on SDS-PAGE (Fig. S5-1 lane 10) to contain monomer with less cleavage compared to the other fractions. This fraction was concentrated down to 32.48 mg/ml using a Microcon[®] Centrifugal Filter (10 kDa) [Millipore] by centrifuging at 3,200 rpm. Both the fraction pool and fraction 42 were from hereon incubated at room temperature. At different time points of incubation (day 1, day 3, etc.) the protein solutions were spun down for one minute at 13,200 rpm and aliquots were taken. Both the fraction pool aliquot and the

fraction 42 aliquots were analyzed with dynamic light scattering and western blotting to monitor time dependent oligomerization.

Dynamic light scattering

Dynamic light scattering (DLS) is a technique that can determine the size distribution of small particles in solution. This is derived from the light scattering that is created when light hits small particles.

For DLS the protein aliquots were diluted in S75 buffer (20 mM Tris and 100 mM NaCl, pH 7.5) to 0.42 mg/ml in a total reaction volume of 50 μ l. A cuvette [Hellma] (105-QS, 300 mm path length) was cleaned with 0.1 M HCl and next with ddH₂O and the protein solution was applied to the cuvette. A size distribution measurement with a Zetasizer Nano S instrument [Malvern Instruments] was performed according to the manufacturer's guide. The results were analyzed and saved on the computer.

Western blotting

For western blot analysis the aliquots were loaded on a SDS-PAGE following the western blot protocol.

2.7 The higher molecular weight protein

2.7.1 Non-specific protein or an ApicalGroEL-A β oligomer

The ~75 kDa protein observed on SDS-PAGE after nickel column purification (Fig. 3-3), could be ApicalGroEL-A β in an oligomeric state or a protein that binds non-specific to the nickel column. To answer this question, the A376 control construct (that does not contain A β) was purified with a nickel column and analyzed on SDS-PAGE. The apical domain of GroEL does not have the propensity to oligomerize on itself. No ~75 kDa molecular weight band should therefore be present in the elution fractions after nickel column purification (analyzed on SDS-PAGE). If there is a ~75 kDa protein band present (on SDS-PAGE) it is most likely a protein that binds non-specific to the nickel column and not ApicalGroEL-A β as an oligomer. The protein composition was further analyzed with western blotting

Western blotting

The fractions containing the most pure ~75 kDa band after nickel column purification were pooled and concentrated down to 23.07 mg/ml using an Amicon Ultra-15 Centrifugal Filter (30 kDa) [Millipore] by centrifuging at 3,000 rpm. The usual western blot protocol was followed.

2.8 General techniques, measurements and preparations

2.8.1 DNA separation by agarose gel

A 1% agarose gel was made by adding 0.5 g agarose in 50 ml 1x TBE buffer (89 mM Tris, 89 mM boric acid and 2 mM EDTA, pH 8.4) [Bio-Rad] and the agarose was dissolved by heating the solution in the microwave and ethidium bromide (0.5 μ g/ml

final concentration) was added. After polymerization the gel was placed into a DNA box and the box was filled with 1x TBE buffer. The DNA sample was mixed with the right volume of 6x loading buffer [Novagen] to make it 1x and loaded into the wells. One lane was loaded with 5 μ l of 0.5-12 kbp. Perfect DNATM Markers [Novagen]. This was run at 90 V for about 45 min to separate the DNA according to size. The DNA was visualized under UV light and a picture was made.

2.8.2 Protein separation by SDS-PAGE

Of each sample 10 μ l was mixed with 12 μ l 2x loading dye (0.04 % bromophenol blue, 1.14 M β -mercaptoethanol, 3.2 % SDS, 32 % glycerol, 0.1 M Tris, pH 6.8), this was boiled for 5 minutes in a 100 °C heating block. Of each sample 15 μ l was loaded on a SDS-PAGE gel to separate the proteins according to their molecular weight.

A CriterionTM Precast Gel (containing 18 or 26 wells) [Bio-Rad] was put into a SDS-PAGE box [Bio-Rad] and the box was filled with 1x TGS (25 mM Tris, 192 mM glycine and 0.1% (w/v) SDS, pH 8.3) The samples were loaded and one lane was loaded with 5 μ l of 10-225 kDa Perfect ProteinTM Markers [Novagen]. The gel was run for 30 minutes at 120 V before the voltage was increased to 150 V for about one hour to separate the proteins according to their molecular weight. Next the gel was put in a staining solution (45 % methanol, 44.9 % mQ 10 % acetic acid and 0.1 % Brilliant Blue R), microwaved for 15 seconds and placed on a rotating platform for 15 minutes. The staining solution was discarded and the gel was put in a destaining solution (50% mQ, 40% methanol and 10% acetic acid) for at least 10 minutes. Now the different molecular weight proteins were visible and a picture was made.

2.8.3 Western blot analysis

The concentration of the protein sample was taken and the desired amount of protein was loaded onto a SDS-PAGE gel following the normal procedure (see section 2.8.2) with the following exceptions. Instead of the normal protein marker 15 μ l prestained marker (Cat. No. 161-0318) [Bio-Rad] was used and the SDS-PAGE was not stained after running. Instead, after disassembling the gel, the sandwich for the protein transfer onto the nitrocellulose membrane was prepared. Two fiber pads [Bio-Rad], two filter papers [Bio-Rad], the SDS-PAGE gel and a nitrocellulose membrane [Bio-Rad] were placed in transfer buffer (25 mM Tris, 192 mM glycine, 20% methanol and 0.1 % SDS, pH 8.3) for 15 minutes. The sandwich apparatus for blotting was prepared and the blot was run at 60 V for 100 min.

After blotting the nitrocellulose membrane was transferred into 50 ml 6 % milk blotting buffer (20 mM Tris, 1 % NaCl, 0.1 % Tween 20 and 6% milk powder, pH 7.5) and put for blocking overnight on a rotating platform. Next day the membrane was washed three times for five minutes each in blotting buffer (20 mM Tris, 1 % NaCl, 0.1 % Tween 20, pH 7.5). Then incubation with one of the primary antibodies took place: α -PolyHistidine (Cat. No. H1029) [Sigma-Aldrich] (1:3000) or α -A β ₁₋₁₆ 6E10 (Cat. No. SIG-39300) [Signet] (1:1000) in 30 ml 2 % milk blotting buffer for two hours on a rotating platform at room temperature. The membrane was washed again three times for five minutes each in blotting buffer and incubated with the secondary antibody α -mouse IgG-Alkaline

Phosphatase (Cat. No. A3562) [Sigma-Aldrich] (1:10,000) in 50 ml 2 % milk blotting buffer for two hours on a rotating platform at room temperature. The membrane was washed again three times for five minutes each in blotting buffer. The substrate BCIP[®]/NBT Alkaline Phosphatase [Sigma-Aldrich] was dissolved in 10 ml mQ in the dark and poured onto the membrane. This was incubated for about 5 minutes till the purple bands appeared; rinsing with an excess of mQ stopped the reaction. Now all the proteins recognized by the antibody were visible as purple bands and a picture was made.

2.8.4 DNA concentration measurement

The DNA concentration was measured using a Nanodrop. The measurements took place at a wavelength of 260 nm. First a blank measurement was made with 1 µl mQ, then 1 µl of the DNA sample was measured, giving the DNA concentration in ng/µl.

2.8.5 Protein concentration measurement

The protein concentration can be calculated by measuring the absorbance with a spectrophotometer at 280 nm. A cuvette with 1 ml flow-through was used as a blank. A dilution of the protein sample with the flow-through was made and the absorbance was measured. The protein concentration was calculated using Beer's Law.

$$\text{Protein concentration} = \frac{A_{280}}{(\epsilon) \cdot (l)} \cdot Mw \cdot \text{dilutionfactor} = \text{mg / ml}$$

The molar extinction coefficient (ϵ) of the different constructs can be found in supplement 8. The path length (l) is 1 cm, the molecular weights (Mw) of the different constructs can also be found in supplement 8.

2.8.6 Bacterial growth measurement

To get an estimation of the amount of bacteria present in solution, the O.D. was measured using a spectrophotometer at 600 nm with LB media as a blank. Next 1 ml of the bacteria culture was measured, resulting in the O.D. of the culture.

2.8.7 LB agar plates

To make LB agar plates, 20 g Difco™ LB Agar, Miller [BD] was dissolved in 500 ml mQ and autoclaved at 120 °C for 20 minutes. The required antibiotic (in this case kanamycin with a final concentration of 100 µg/ml) was added to the agar media when the temperature had cooled down to ~55 °C. About 20 ml of LB agar was poured into each plate and left to solidify. The plates were stored at 4 °C.

2.8.8 LB cultures

To make LB cultures, 12.5 g Difco™ LB Broth, Miller [BD] was dissolved in 500 ml mQ, split in 10 ml aliquots and autoclaved at 120 °C for 20 minutes.

2.8.9 LB media

To make LB media, 10 g NaCl, 10 g Bacto™ Tryptone and 5 g Bacto™ Yeast Extract were dissolved in 1 L mQ and autoclaved at 120 °C for 25 minutes.

2.9 Apparatus

- Centrifuges:
 - Sorvall RC-5B [DuPont Instruments]
 - Sorvall RC 3B [DuPont Instruments]
 - GS-6R [Beckman]
- Eppendorf centrifuge: 5415D [Eppendorf]
- FPLC:
 - System: LCC-501 Plus controller [Pharmacia Biotech]
 - UV detector: UV-MII [Pharmacia Biotech]
 - Pump: LKB Pump P-500 [Pharmacia Biotech]
 - Fraction collector: FRAC-100 [Pharmacia Biotech]
- French Press: [Sim-amico spectronic instruments]
- Gel documentation: Gel Doc XR [Bio-Rad]
- Incubator 37 °C: 1500E [VWR]
- Mass spectrometer: Axima-CFR instrument [Kratos analytical]
- Nanodrop: ND-1000 [Nanodrop®]
- PCR machine: GeneAmp PCR system 2400 [Perkin Elmer]
- pH-electrode: Orion 9156APWP AquaPro [Thermo scientific]
- pH-meter: PerpHecT® digital LogR™ meter [Thermo scientific]
- Shaker: [New Brunswick Scientific]
- Spectrophotometer: Cary 50 [Varian]
- SpeedVac: SVC 100H [Savant]
- Waterbath 37 °C: [Fisher Scientific]
- Waterbath 42 °C: 1203 [VWR]
- Dynamic light scattering: Zetasizer Nano S instrument [Malvern Instruments]

Chapter 3; Results

3.1 General results

3.1.1 Cloning of the ApicalGroEL-A β constructs

The constructs were confirmed by performing a PCR on the plasmid DNA with insert specific primers. The amplification products were run on an agarose gel (Fig. 3-1). In addition, the constructs were confirmed by sequencing (Tab. 3-1 and supplement 8). Fig. 3-1 shows linker amplification at the expected size.

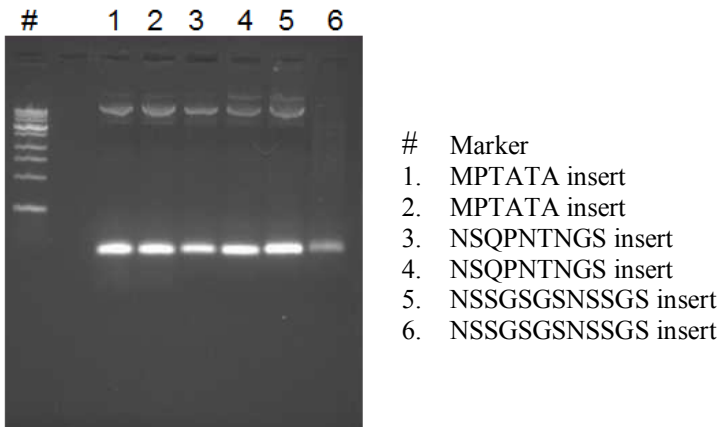


Figure 3-1 Agarose gel of PCR amplification products. The amplification products were run on the gel to see if the linkers were inserted.

Construct	Sequence confirmed	Soluble at 18 °C	Purified
A376-SAG-A β 42	Yes	No	No
A376-6SAG-A β 42	Yes	Yes	Yes
A376-9SAG-A β 42	Yes	Yes	Yes
A376-12SAG-A β 42	Yes	Yes	No
A376-6MPT-A β 42	Yes	Yes	Yes
A376-9NSQ-A β 42	Yes	Yes	Yes
A376-12NSS-A β 42	Yes	Yes	No
A376-6SAG-A β 17-42	Yes	Yes	Yes
A336-6SAG-A β 42	Yes	Yes	Yes
A336-12GSA-A β 42	Yes	Yes	Yes
A336-6SAG-A β 17-42	Yes	Yes	Yes
A376 control	Yes	Yes	Yes
A336 control	Yes		No

Table 3-1 ApicalGroEL-A β constructs and experiments.

3.1.2 Expression of the ApicalGroEL-A β constructs

To test the solubility of the protein constructs, expression tests at 37 °C and 18 °C were performed. Expression at 18 °C shows ApicalGroEL-A β expressed in soluble fraction (supernatant) at ~25 kDa (Fig. 3-2) while expression at 37 °C did not show

ApicalGroEL-A β in the soluble fraction. This was consistent for all ApicalGroEL-A β constructs except for A376-SAG-A β 42, which was insoluble at 37 °C as well as at 18 °C (Tab. 3-1). Thus for purification, the ApicalGroEL-A β constructs were expressed at 18 °C.

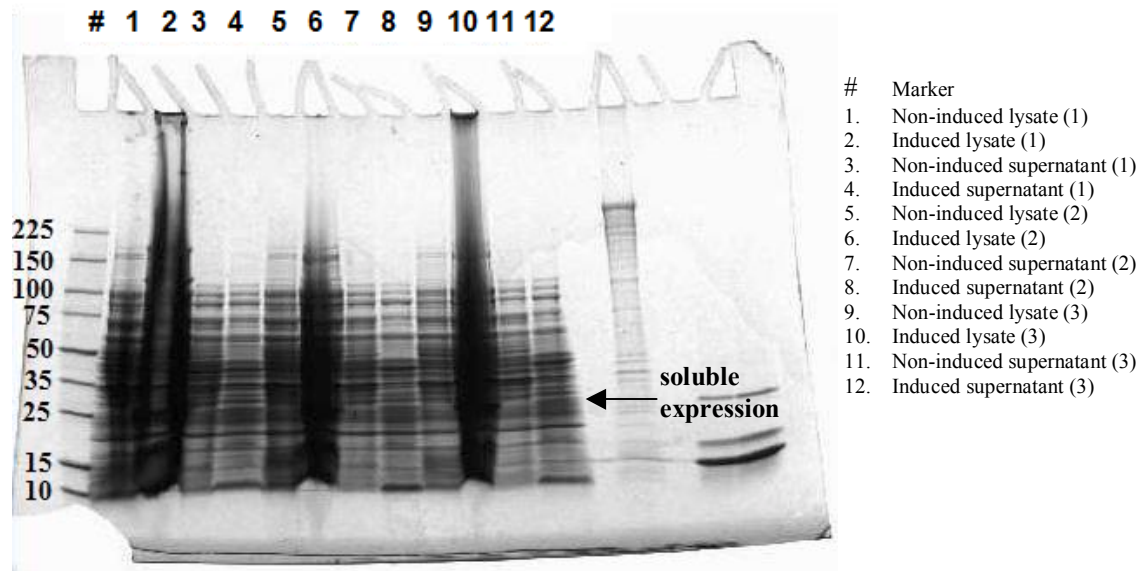


Figure 3-2 SDS-PAGE of an expression test at 18 °C. Non-induced and induced, lysate and supernatant were run on the SDS-PAGE to see if the constructs were soluble. (1) A376-6SAG-A β 42, (2) A376-9SAG-A β 42 and (3) A376-12SAG-A β 42. The last five lanes contain protein samples of other experiments.

3.1.3 Purification of the ApicalGroEL-A β constructs

The ApicalGroEL-A β constructs showed a similar affinity for nickel column purification, most of our protein eluted between 27 mM and 169 mM imidiazole. The chromatograms showed a small peak very early during the elution protocol containing non-specific proteins and a broad peak for ApicalGroEL-A β (Fig. S3-1).

On the SDS-PAGEs three observations were made that were found to be the same for all ApicalGroEL-A β constructs that have been purified (Fig. 3-3). First, ApicalGroEL-A β was visible as a monomer (~25 kDa). Second, there were small protein bands of ~10-20 kDa. These proteins could be degradation products of ApicalGroEL-A β or non-specific proteins that bind to the nickel column. The last observation was a ~75 kDa protein, this could be ApicalGroEL-A β in an oligomeric state, maybe as a trimer ($3 \times 25 = 75$), or it could be a non-specific protein that bind to the nickel column.

Based on these three observations the experiments were divided based on oligomeric state. The first approach has been to isolate ApicalGroEL-A β as monomer and screen for crystallization. The assumption was made that the construct isolated as a monomer would crystallize in an oligomeric state, since A β has the propensity to oligomerize at high concentration¹⁷ (section 1.1.6). The second approach has been to isolate ApicalGroEL-A β in an oligomeric state and to crystallize the protein in this oligomeric state. The ApicalGroEL-A β monomer was purified, brought to high concentration and incubated to see if it would form oligomers in a time dependent manner, which can be purified and

crystallized. Besides these two approaches, the ~75 kDa protein was analyzed to figure out if it was an oligomer of our protein or non-specific protein.

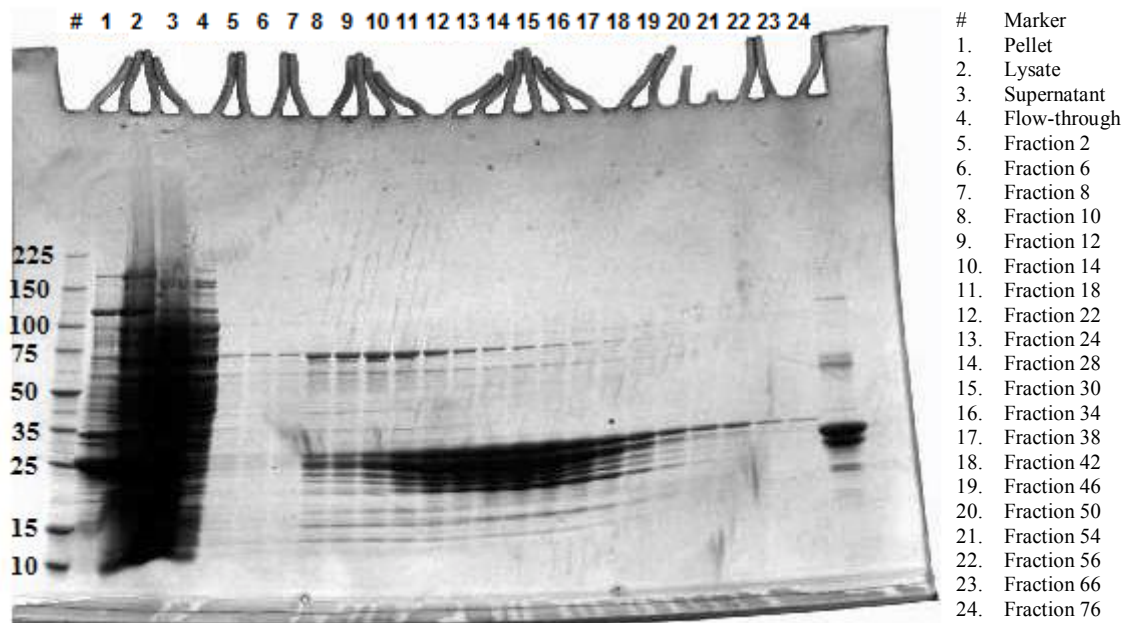


Figure 3-3 SDS-PAGE of a nickel column purification of A376-6MPT-Aβ42. The last lane contains a protein sample of another experiment.

3.2 ApicalGroEL-Aβ isolation as a monomer

3.2.1 Crystallization

All the ApicalGroEL-Aβ constructs that were screened for crystallization formed crystals within a few days (Fig. 3-4). For four different constructs crystallization was optimized to grow higher quality crystals. Multiple datasets were collected. Four higher quality datasets extending beyond 3.0 Å of three different constructs were solved with molecular replacement (Tab. 3-2). The apical domain of GroEL (PDB ID code: 1KID) was used as a search model. The search model crystallized in the orthorhombic space group $P2_12_12_1$, with unit-cell parameters $a = 47.72 \text{ \AA}$ $b = 63.81 \text{ \AA}$ $c = 75.10 \text{ \AA}$ and contained one monomer per asymmetric unit³⁹.

Construct	Crystallization screening	Crystals	Optimized	Solved
A376-6SAG-Aβ42	Yes	Yes	Yes	Yes (2x)
A376-9SAG-Aβ42	Yes	Yes	Yes	No
A376-6MPT-Aβ42	Yes	Yes	Yes	Yes
A376-9NSQ-Aβ42	Yes	Yes	Yes	No
A376-6SAG-Aβ17-42	Yes	Yes	No	Yes
A336-6SAG-Aβ42	Yes	Yes	No	No

Table 3-2 ApicalGroEL-Aβ constructs and crystal formation.

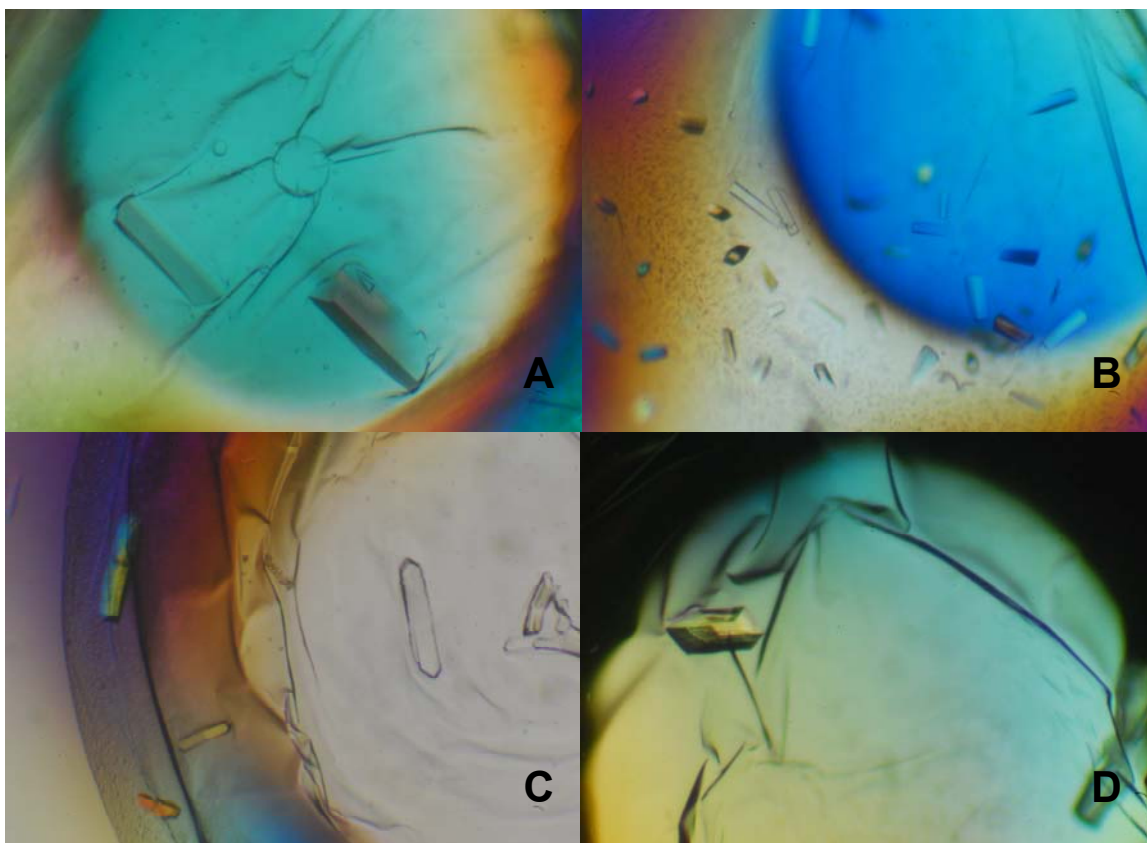


Fig. 3-4 Crystals under polarized light. (A) A376-6SAG-A β 42 crystals in Wizard screen I condition 31. (B) A376-6SAG-A β 42 crystals in PEG/ION I condition 12. (C) A376-6MPT-A β 42 crystals in Crystal screen I condition 6. (D) A376-6SAG-A β 17-42 crystals in Crystal screen II condition 5.

A376-6SAG-A β 42 structure 1

The crystals were initially found in the crystallization solution PEG/ION I condition 12: 0.2 M Ammonium Iodide, 20% (w/v) Polyethylene Glycol 3350, pH 6.2. The starting protein concentration was 8.8 mg/ml in dialysis buffer containing 20 mM Tris, 100 mM NaCl and 5% glycerol, pH 7.5.

The crystals belonged to the orthorhombic space group $P2_12_12_1$, with unit-cell parameters $a = 49.63 \text{ \AA}$, $b = 63.25 \text{ \AA}$ and $c = 75.52 \text{ \AA}$ and contained one monomer per asymmetric unit. The crystals diffracted to 2.19 \AA .

Based upon the diffraction pattern and the intensity of the spots (Fig. 3-5), along with known phase information the protein structure was solved. After model building and refinement the electron density map showed electron density up to the last residue of the apical domain of GroEL (V376). However, no connected and continuous electron density for the linker and A β was observed, which should have been present after the C-terminus of the apical domain. Also, no connected and continuous electron density for the N-terminal His-tag was observed. Figure 3-6 shows the solved structure, the apical domain of GroEL (residues 191-376 of GroEL).

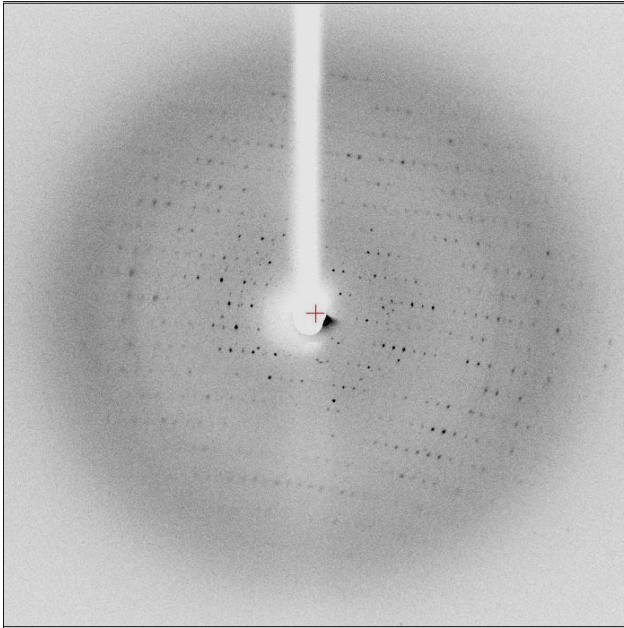


Figure 3-5 A X-ray diffraction pattern of crystallized A376-6SAG-A β 42 protein.

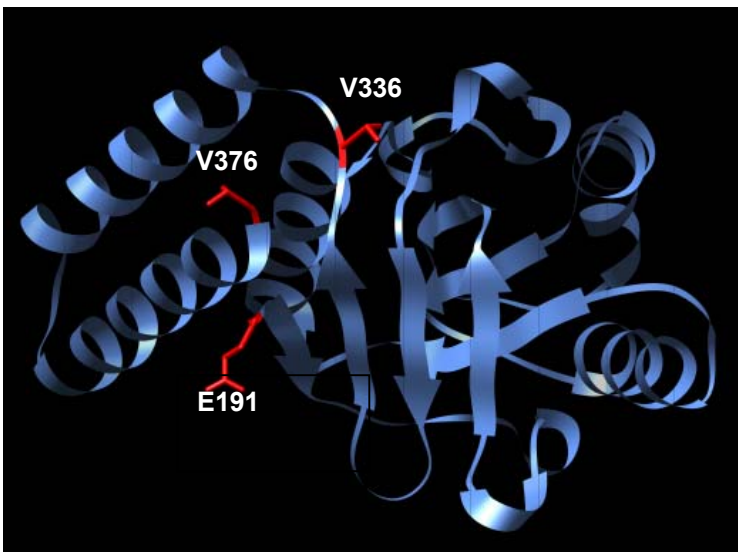


Figure 3-6 The solved structure of A376-6SAG-A β 42, the apical domain of GroEL. Image generated in Chimera.

A376-6SAG-A β 42 structure 2

The crystals were initially found in the crystallization solution Wizard screen I condition 31: 200 mM NaCl, 20% (w/v) Polyethylene Glycol 8000 and 0.1 M phosphate-citrate, pH 4.2. The starting protein concentration ranged from 8.8 mg/ml to 10.6 mg/ml in dialysis buffer containing 20 mM Tris, 100 mM NaCl and 5% glycerol, pH 7.5.

The crystals belonged to the orthorhombic space group $P2_12_12_1$, with unit-cell parameters $a = 55.63 \text{ \AA}$, $b = 65.35 \text{ \AA}$ and $c = 75.63 \text{ \AA}$ and contained one monomer per asymmetric unit. The crystals diffracted to 2.28 \AA .

After model building and refinement the electron density map showed electron density up to the last residue of the apical domain of GroEL (V376) (Fig. 3-7). Some connected density was visible after the C-terminal residue of the apical domain for the first few residues of the linker (Fig. 3-7 *). However, this density was not continuous there was no electron density for A β . Also, no continuous electron density for the N-terminal His-tag was observed.

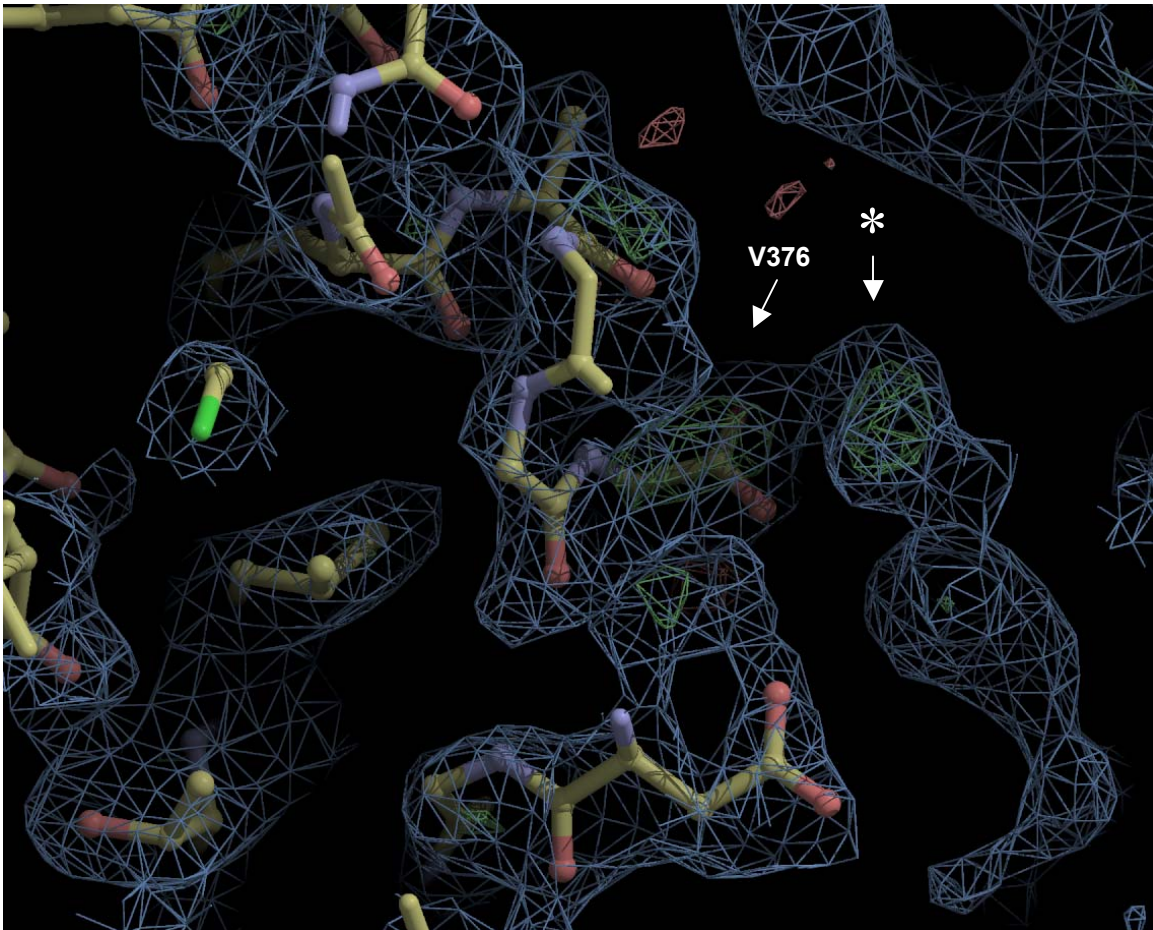


Figure 3-7 Electron density map (blue) of A376-6SAG-A β 42. The residues of the apical domain were built into the density. Negative density is red and positive density is green. Carbon atoms are yellow, nitrogen atoms are blue and oxygen atoms are red. Image generated in Coot. (*) Connected density after the C-terminal residue (V376) of the apical domain.

A376-6MPT-A β 42 structure

The crystals were initially found in the crystallization solution Crystal screen I condition 6: 0.2 M Magnesium Chloride hexahydrate, 30% (w/v) Polyethelene glycol 4000 and 0.1 M Tris Hydrochloride, pH 8.5 The starting protein concentration was 6 mg/ml in dialysis buffer containing 20 mM Tris and 100 mM NaCl, pH 7.5.

The crystals belonged to the orthorhombic space group $P22_12_1$, with unit-cell parameters $a = 35.26 \text{ \AA}$, $b = 76.20 \text{ \AA}$ and $c = 83.88 \text{ \AA}$ and contained one monomer per asymmetric unit. The crystals diffracted to 2.00 \AA .

After model building and refinement the electron density map showed electron density up to the last residue of the apical domain of GroEL. However, no connected and continuous

electron density for the linker and A β was observed and no connected and continuous electron density for the N-terminal His-tag was observed.

A376-6SAG-A β 17-42 structure

The crystals were initially found in the crystallization solution Crystal screen II condition 5: 2.0 M Ammonium Sulfate and 5% (v/v) iso-propanol. The starting protein concentration ranged from 15.94 to 19.25 mg/ml in dialysis buffer containing 20 mM Tris and 100 mM NaCl, pH 7.5.

The crystals belonged to the orthorhombic space group $P2_12_12$, with unit-cell parameters $a = 72.43 \text{ \AA}$, $b = 76.59 \text{ \AA}$ and $c = 35.05 \text{ \AA}$ and contained one monomer per asymmetric unit. The crystals diffracted to 2.69 \AA .

After model building and refinement the electron density map showed electron density up to the last residue of the apical domain of GroEL. However, no connected and continuous electron density for the linker and A β was observed. Also, no connected and continuous electron density for the N-terminal His-tag was observed.

3.2.3 Monomer cleavage analysis

The smaller molecular weight bands of $\sim 10\text{-}20 \text{ kDa}$ that were observed on SDS-PAGEs (Fig. 3-3) of nickel column purifications were suggested to be cleavage products of ApicalGroEL-A β . To analyze these cleavages mass spectrometry and western blotting was used.

Mass spectrometry

Mass spectrometry analysis suggested that there was some cleavage happening (Fig. 3-8). The single and double charge peaks each gave multiple mass/charge results. For example the single charge peak in Figure 3-8 gave mass/charge results of 21287, 21239 and 21039. The mass spectrometry data indicates that there were different protein sizes present. A uniform population would have given a sharp peak. This indicates that there is most likely not a uniform population of our protein present, but cleaved and uncleaved protein.

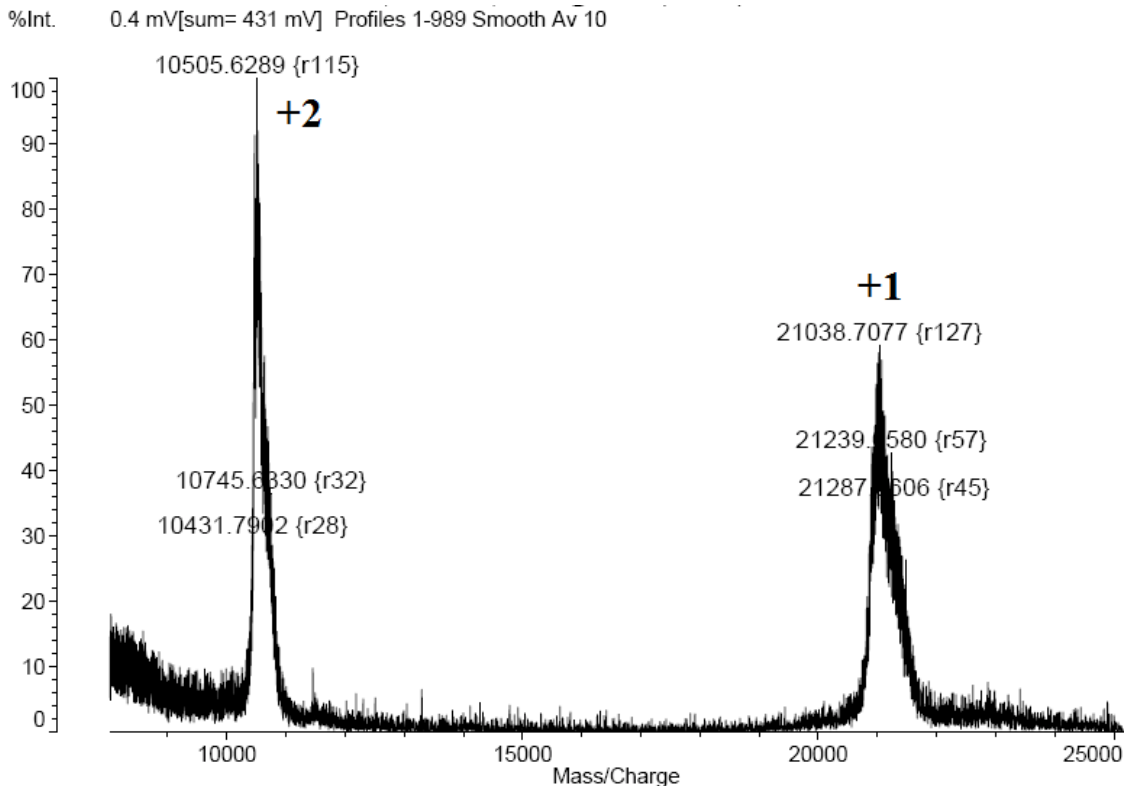


Figure 3-8 Mass spectrometry of A336-6SAG-A β 42. The +2 peak is the double charged protein and the +1 peak is the single charged protein. Plotted on the y-axis is the relative intensity. This is the relative intensity to the tallest peak in the spectrum with the tallest peak set to 100 %. Plotted on the x-axis is the mass divided by the charge.

Western blotting

Western blot analysis of the protein suggested that the observed smaller molecular weight bands of 10-20 kDa are degradation products of ApicalGroEL-A β , because the α -A β ₁₋₁₆ antibody recognized these bands (Fig. 3-11 A the fraction pool at different time points of incubation). They are C-terminal cleavage products (the C-terminus is where A β is situated) since the bands of 10-20 kDa were α -His-tag negative and α -A β ₁₋₁₆ positive (Fig. 3-11 A and B the fraction pool at different time points of incubation). A β itself is only 4.5 kDa the observed proteins bands were between 10-20 kDa, it must have been a small C-terminal fragment (about the size of A β) that was cleaved off since ApicalGroEL-A β is only 25 kDa and no 10-15 kDa α -His-tag positive bands were observed. Apparently A β started to self-assemble immediately after cleavage.

3.2.4 Crystal composition analysis

Western blotting

The composition of the crystals was analyzed with western blotting to see if A β was present. The crystals showed a ~25 kDa band (monomer = 28.3 kDa) that was α -His-tag and α -A β ₁₋₁₆ positive (Fig. 3-9 lanes 8 and 9), suggesting that the crystals were formed of ApicalGroEL-A β that contained the whole apical domain and at least A β ₁₋₁₆. The high molecular weight α -His-tag and α -A β ₁₋₁₆ positive bands at ~40 kDa (dimer = 56.6 kDa),

~75 kDa (trimer = 84.9) and ~100 kDa (tetramer = 113.2 kDa) were assumed to be the protein monomer that self-assembles after dissolving of the crystals.

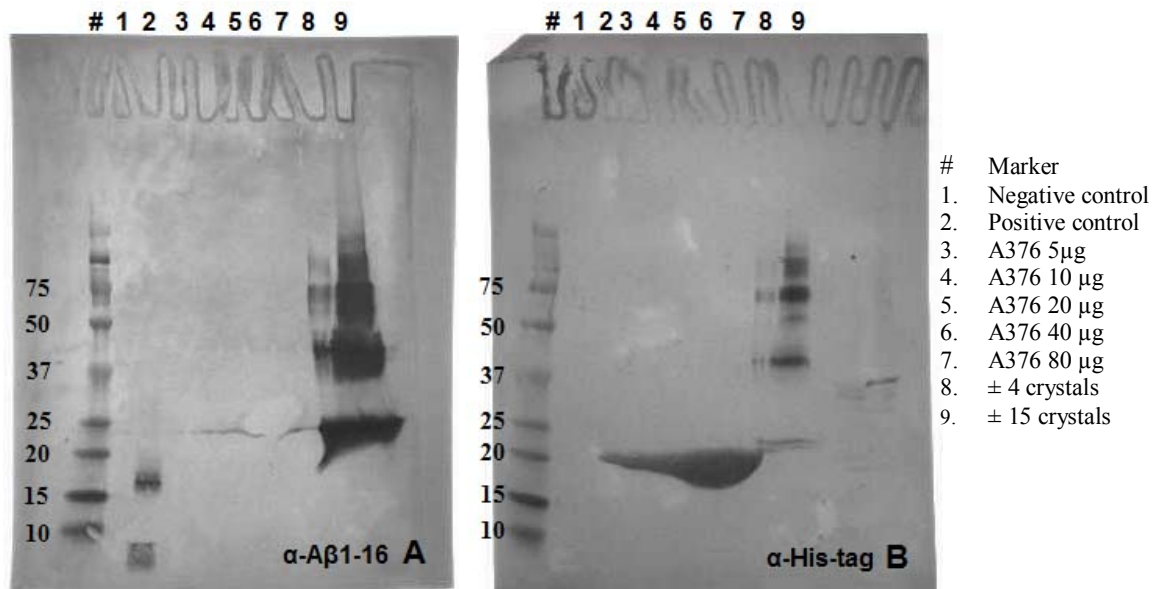


Figure 3-9 Western blots of A376-6SAG-Aβ₄₂ crystals and A376 control protein. 5 μg of the negative control PKS11 protein without a His-tag (35 kDa), 0.08 μg of the positive control synthetic Aβ₄₂ (4.5 kDa) (Cat. No. A-1002-1) [rPeptide], different amounts of A376 control protein and different amounts of A376-6SAG-Aβ₄₂ crystals were applied to a nitrocellulose membrane. (A) Nitrocellulose membrane probed with α-Aβ₁₋₁₆ 6E10 (1:1000). (B) Nitrocellulose membrane probed with α-PolyHistidine (1:3000). The last four lanes contain samples of other experiments.

3.3 ApicalGroEL-Aβ isolation as an oligomer

3.3.1 Time dependent oligomerization analysis

In order to isolate and crystallize ApicalGroEL-Aβ in an oligomeric state the protein monomer was purified and brought to high concentration to see if it would form oligomers in a time dependent manner that could be isolated and crystallized.

This approach is inspired by the fact that Aβ oligomerization is known to be concentration and time dependent¹⁷ (section 1.1.6). To monitor the time dependent oligomerization of ApicalGroEL-Aβ, the aliquots of ApicalGroEL-Aβ at different time points of incubation were analyzed with dynamic light scattering and western blotting.

Dynamic light scattering

The DLS data for both the fraction pool (Fig. S4-1) and fraction 42 (less cleaved fraction) (Fig. 3-10) indicated time dependent oligomerization. The oligomerization was indicated by an increase of intensity of the bigger diameter peak, which was suggested to be a higher order assembly of ApicalGroEL-Aβ or aggregate. At the same time the intensity of the smaller diameter peak was decreasing, this was suggested to be the protein monomer. This pattern was clearer for fraction 42 than it was for the fraction pool.

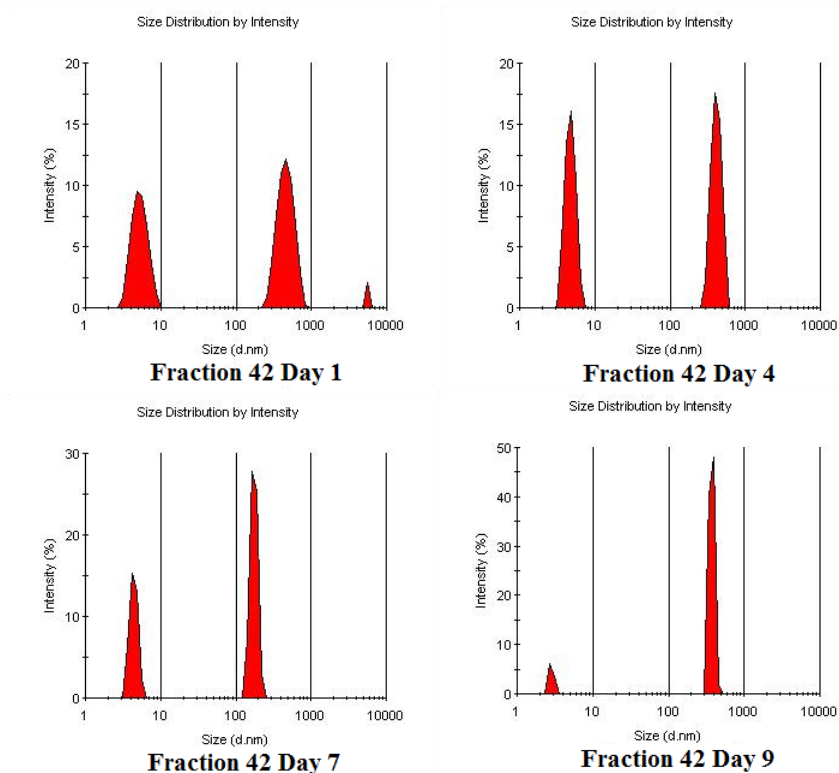


Figure 3-10 Dynamic light scattering of fraction 42 of A336-6SAG-A β 42 at different time points of incubation. On the y-axis is the relative intensity of the scattered light plotted. On the x-axis is the distribution of the different sizes (diameter in nanometer: d.nm) plotted.

Western blotting

The western blots (Fig. 3-11) clearly supported the dynamic light scattering data for fraction 42 (less cleaved fraction); as indicated by the increase of ApicalGroEL-A β present at ~50 kDa (dimer = 47.8 kDa), ~75 kDa (trimer = 71.7 kDa) and ~100 kDa (tetramer = 95.6 kDa) in a time dependent manner. The ~75 kDa band observed with the α -A β ₁₋₁₆ antibody was not observed with the α -His-tag antibody, that could be due to a not high enough sensitivity of the α -His-tag antibody, or due to α -A β ₁₋₁₆ binding non-specific to a ~75 kDa protein.

This time dependent oligomerization pattern could not be confirmed for the fraction pool. The presence of an oligomer at ~40 kDa both α -A β ₁₋₁₆ and α -His-tag positive was observed, which is consistent with a dimer with part of A β cleaved off. Also, an α -A β ₁₋₁₆ positive band at ~80 kDa was observed for the fraction pool. This is consistent with a partially cleaved tetramer; C-terminal with part of A β cleaved of or N-terminal since the band was not observed with the α -His-tag antibody, but again this could be due to a not high enough sensitivity of the α -His-tag antibody, or due to α -A β ₁₋₁₆ binding non-specific to a ~75 kDa protein.

The lack of time dependent oligomerization for the fraction pool (no increase of protein present at higher molecular weights over time) could be due to fact that ApicalGroEL-A β is being cleaved and this inhibited oligomerization.

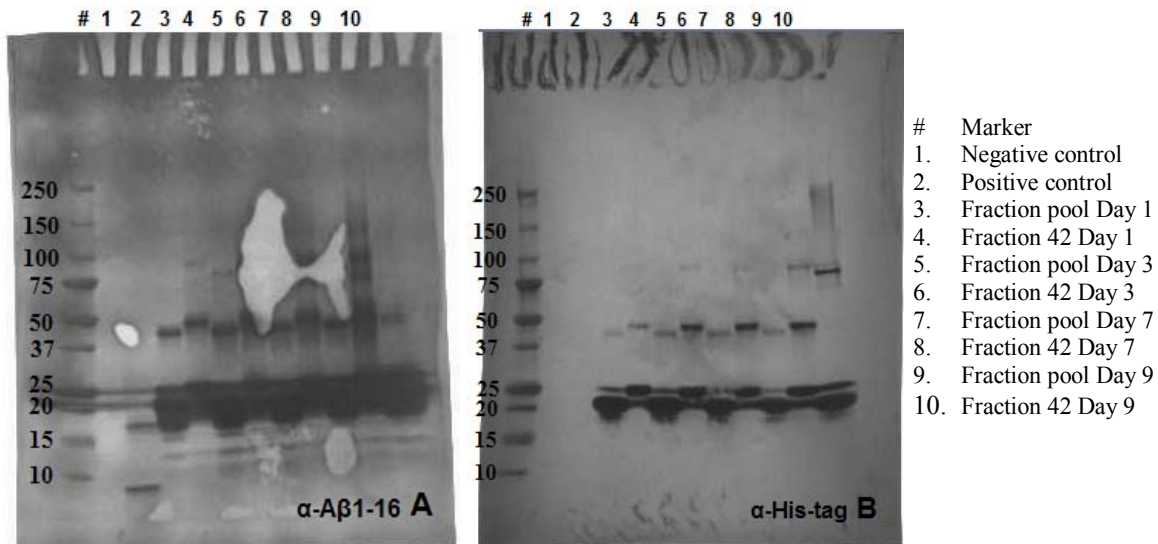


Figure 3-11 Western blots of A336-6SAG-A β 42 monitoring time dependent oligomerization. 5 μ g of the negative control PKS11 protein without a His-tag (35 kDa) and 0.08 μ g of the positive control synthetic A β ₄₂ (4.5 kDa) (Cat. No. A-1002-1) [rPeptide] were applied to a nitrocellulose membrane. Together with 5 μ g of the fraction pool and 5 μ g of fraction 42 at different time points of incubation. (A) Nitrocellulose membrane probed with α -A β ₁₋₁₆ 6E10 (1:1000). (B) Nitrocellulose membrane probed with α -

3.4 The higher molecular weight protein

3.4.1 Non-specific protein or an ApicalGroEL-A β oligomer

The ~75 kDa protein observed on SDS-PAGE after nickel column purification (Fig. 3-3), could be ApicalGroEL-A β in an oligomeric state, or a non-specific protein that bind to the nickel column. This protein was analyzed on SDS-PAGE and with western blotting.

SDS-PAGE analysis

The apical only construct (A376 control) that does not contain A β was purified to see whether the observed band at ~75 kDa (Fig. 3-3) is dependent on the presence of A β or not. A ~20 kDa and a ~75 kDa band were observed on SDS-PAGE (Fig. 3-13). Thus the presence of the ~75 kDa protein was not dependent on the presence of A β . The apical domain of GroEL does not have the propensity to oligomerize on itself, suggesting that the ~75 kDa protein was a non-specific protein that bind to the nickel column and not an ApicalGroEL-A β oligomer.

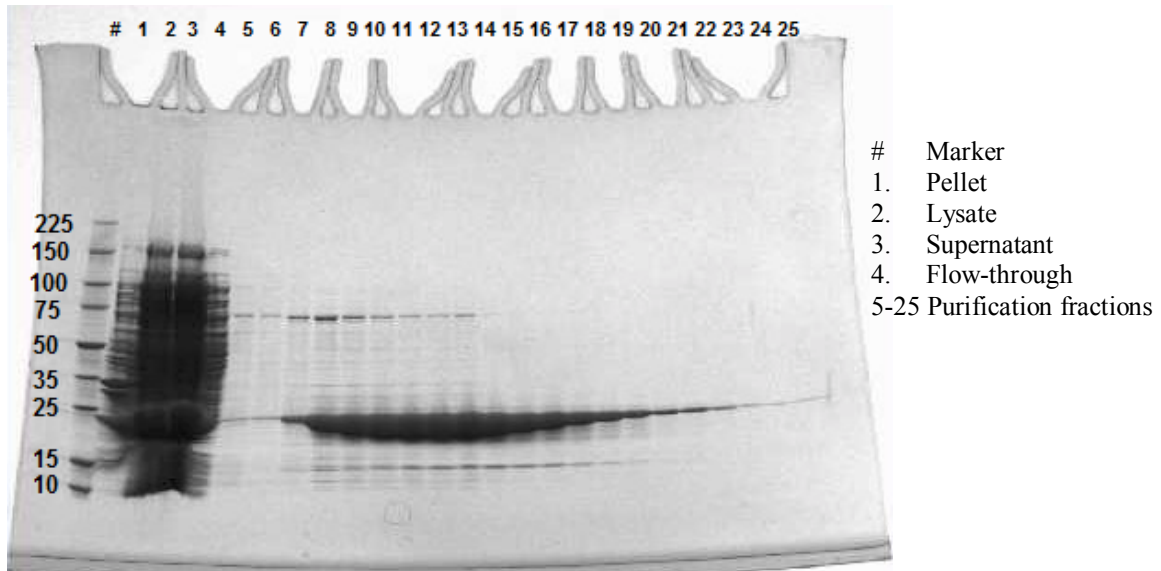


Figure 3-13 SDS-PAGE of a nickel column purification of A375 control.

Western blotting

Western blot analysis of the A376 control purification supported the hypothesis that the ~75 kDa protein is a non-specific protein. The western blots (Fig. 3-9 lanes 3-7) showed a α -His-tag positive band at ~20 kDa (monomer = 22.9 kDa). No ~75 kDa band was recognized by the α -His-tag antibody. The ~75 kDa protein is thus confirmed to lack a His-tag, which is in contrast to our His-tagged protein. This suggests that the ~75 kDa protein was not an oligomer of our protein. The α -A β_{1-16} antibody did not detect any A β , which is consistent with A β not being present in this construct.

Chapter 4; Discussion and conclusion

More and more evidence indicates that especially the soluble A β oligomers are neurotoxic and play an important role in the Alzheimer's disease related pathology^{4,5,23,25}. Therefore the ultimate aim of this study was to solve the structure of human A β ₄₂ in an oligomeric state for rational structure based drug design against Alzheimer's disease.

4.1 ApicalGroEL-A β isolation as a monomer

To solve the structure of A β , the monomeric state of the different ApicalGroEL-A β constructs has been purified and crystallized. The crystals that were obtained had similar unit cell dimensions as the search model, the apical domain of GroEL in a monomeric state (PDB ID code: 1KID), which was used for molecular replacement to get the phase information. This indicates that ApicalGroEL-A β does not oligomerize in the crystal, since that would result in different unit cell dimensions. Most likely the protein is present as a monomer in the unit cell.

Variations in apical domain size, linker length and hydrophobicity, and A β size did not seem to change important characteristics. All ApicalGroEL-A β constructs showed the same purification and crystallization pattern. The four electron density maps (from three different constructs) that were obtained showed electron density up to the last residue of the apical domain. No continuous electron density was observed for the linker and A β . A few possible reasons for the absence of electron density are suggested.

A crystal is composed of molecules arranged in an ordered three-dimensional array³⁷. It is possible that the crystals are composed of an ordered array of cleaved ApicalGroEL-A β monomer that does not contain A β . This is a realistic hypothesis since cleavage seems to be a problem in this study. When analyzing the protein with western blotting the presence of His-tag and at least A β ₁₋₁₆ is confirmed. However, small (10-20 kDa) protein bands that are α -A β ₁₋₁₆ positive are also observed, these are thought to be C-terminal cleavage products of our protein. This is further supported by mass spectrometry that indicates presence of different sizes of ApicalGroEL-A β . Though, when analyzing the composition of the crystals with western blots the presence of at least A β ₁₋₁₆ in the crystals was confirmed. So the observed cleavage seems unlikely to be the reason for the missing electron density for A β .

It can also be due to the lack of three-dimensional periodicity because of too much flexibility of A β in the unit cell. In other words, perhaps A β is not present at the same place in every unit cell, which results in positional disorder³⁷. This is most likely the reason for the absent density for the N-terminal His-tag.

Another possibility is that A β is in a disordered conformation itself. It was hypothesized that removing of the first 16 residues of A β (the residues that are known to be disordered¹⁶) would lead to a better electron density map. However the electron density map of A376-6SAG-A β 17-42 did not show continuous density for A β either.

It can also be due to the fact that A β is at the C-terminus of the construct; it is not uncommon for residues at termini to be missing from a model³⁷. To conclude, in this approach we seem to be able to purify and crystallize ApicalGroEL-A β as a monomer. The next step is to find a solution for the missing electron density for A β .

4.2 ApicalGroEL-A β isolation as an oligomer

The ApicalGroEL-A β monomer at high concentration assembles into higher order assemblies in a time dependent manner, as indicated by dynamic light scattering and western blot analysis. This observation is supported by work of others¹⁷. However, when the ApicalGroEL-A β monomer is being cleaved, time dependent oligomerization seems to be inhibited significantly.

It is inconclusive what the sizes of the formed oligomers are, since SDS-PAGE can only display the estimated molecular weight of a denatured protein.

4.3 The higher molecular weight protein

The ~75 kDa protein observed on SDS-PAGE after nickel column purification is most likely not ApicalGroEL-A β in an oligomeric state but a protein that binds non-specifically to the nickel column. The apical domain of GroEL does not have the propensity to oligomerize on itself. However, the same band was observed when purifying the A376 control protein (that does not contain A β), confirming that the ~75 kDa protein is not dependent on the presence of A β . In addition, the ~75 kDa protein was not recognized by the α -His-tag antibody and thus is confirmed to be lacking a His-tag, which is in contrast to our His-tagged protein.

4.4 Suggestions for further research

Further research would continue on experiments to isolate ApicalGroEL-A β as a monomer and to find ways to get electron density for A β . One can think of making constructs that allow less flexibility for A β , to make sure that A β is present at the same location in every unit cell. Also one can try to use multiple techniques to solve the phases, one way could give better results than the other one. Or maybe a combination of techniques would work. For example combining experimental phase information from anomalous scattering with molecular replacement phases.

Since we cannot totally exclude the possibility that A β is just not present in the crystal as a result of cleavage processes, it would also be recommended to prevent as much cleavage from happening as possible by increasing the concentration of protease inhibitors during purification.

Further research would also continue on experiments to isolate ApicalGroEL-A β in an oligomeric state. A promising way to do this seems to be the incubation of the monomer to make it assemble to an oligomeric state over time. Once oligomers are starting to form (which can be monitored with dynamic light scattering) they can be purified with size exclusion chromatography and crystallized. Heretofore any cleavage processes should be tried to be prevented, since that is shown to inhibit oligomerization.

An interesting question to answer would be whether this approach (purifying and crystallizing an oligomeric state) is feasible. Oligomers exist in equilibrium with the monomer¹⁹. So when an oligomeric state is separated from the other states in solution this may trigger disassembly. An oligomeric state is not easily preserved so it can be quite difficult to isolate and crystallize and if one succeeds it could still be hard to reproduce.

The best approach would be to try to isolate and crystallize the smaller size oligomers (dimers and trimers) since these are stable^{23,24}.

4.5 Concluding statement

Linking A β to the apical domain of GroEL offers advantages; the ApicalGroEL-A β protein is soluble and easy to purify and crystallize. In addition the apical domain of GroEL itself does not oligomerize, therefore a stable oligomer formed is due to the presence of A β . One must keep in mind to preserve the ability of A β to fold into its native conformation, since the goal is to design drugs that will target that structure *in vivo*.

Unfortunately it was not possible to solve an oligomer structure of A β yet. However there are still multiple approaches that can be tried, hopefully one of them will eventually enable us to solve the structure of A β in an oligomeric state; thereby making it possible to design drugs that specifically target A β oligomers and help to win the fight against Alzheimer's disease.

References

1. Chiti, F. and Dobson, C. M. Protein misfolding, functional amyloid and human disease. *Annu. Rev. Biochem.* 75: 333-366 (2006).
2. Eisenberg, D., Nelson, R., Sawaya, M. R., Balbirnie, M., Sambashivan, S., Ivanova, M. I., Madsen, A. Ø. and Riek, C. The structural biology of protein aggregation diseases: fundamental questions and some answers. *Acc. Chem. Res.* 39: 568-575 (2006).
3. Haass, C. and Selkoe, D. J. Soluble protein oligomers in neurodegeneration: lessons from the Alzheimer's amyloid β -peptide. *Moll. Cell Bio.* 8: 101-112 (2007).
4. Townsend, M., Shankar, G. M., Mehta, T., Walsh, D. M. and Selkoe, D. J. Effects of secreted oligomers of amyloid β -protein on hippocampal synaptic plasticity: a potent role for trimers. *J. Physiol.* 572.2: 477-492 (2006).
5. Zhang, Y., McLaughlin, R., Goodyer, C. and LeBlanc, A. Selective cytotoxicity of intracellular amyloid β peptide₁₋₄₂ through p53 and Bax in cultured primary human neurons. *J. Cell. Bio.* 156: 519-529 (2002).
6. Cummings, B.J., Pike, C.J., Shankle, R. and Cotman, C. W. β -amyloid deposition and other measures neuropathology predict cognitive status in Alzheimer's disease. *Neurobiol. Aging.* 17:921-933 (1996).
7. Harper, J. D., Wong, S. S., Lieber, C. M. and Lansbury, P. T. Assembly of A β amyloid protofibrils: an in vitro model for a possible early event in Alzheimer's disease. *Biochem.* 38: 8972-8980 (1999).
8. Kuo, Y., Emmerling, M. R., Vigo-Pelfrey, C., Kasunic, T. C., Kirkpatrick, J. B., Murdock, G. H., Ball, M. J. and Roher, A. E. Water-soluble A β (N-40, N-42) oligomers in normal and Alzheimer disease brains. *J. Biol. Chem.* 271: 4077-4081 (1996).
9. Lue, L. F., Kuo, Y. M., Roher, A. E., Brachova, L., Shen, Y., Sue, L., Beach, T., Kurth, J. H., Rydel, R. E. and Rogers, J. Soluble amyloid beta peptide concentrations as a predictor of synaptic change in Alzheimer's disease. *Am. J. Pathol.* 155: 853-862 (1999).
10. Glenner, G. G. and Wong, C. W. Alzheimer's disease: initial report of the purification and characterization of a novel cerebrovascular amyloid protein. *Biochem. Biophys. Res. Commun.* 120: 885-890 (1984).
11. Kang, J., Lemaire, H. G., Unterbeck, A., Salbaum, J. M., Masters, C. L., Grzeschik, K. H., Multhaup, G., Beyreuther, K. and Müller-Hill, B. The precursor of Alzheimer's disease amyloid A4 protein resembles a cell-surface receptor. *Nature.* 325: 733-736 (1987).
12. Selkoe, D. J. Normal and abnormal biology of the β -amyloid precursor protein. *Annu. Rev. Neurosci.* 17: 489-517 (1994).
13. Haass, C. Take five—BACE and the c-secretase quartet conduct Alzheimer's amyloid β -peptide generation. *EMBO J.* 23: 483-488 (2004).
14. Verdile, G., Fuller, S., Atwood, C. S., Laws, S. M., Gandy, S. E. and Martins, R. N. The role of beta amyloid in Alzheimer's disease: still a cause of everything or the only one who got caught? *Pharmacol. Res.* 50: 397-409 (2004).

15. Coles, M., Bicknell, W., Watson, A. A., Fairlie, D. P. and Craik, D. J. Solution structure of amyloid β -peptide(1-40) in a water—micelle environment. Is the membrane-spanning domain where we think it is? *Biochem.* 37: 11064-11077 (1998).
16. Zirah, S., Kozin, S. A., Mazur, A. K., Blond, A., Cherminant, M., Ségalas-Milazzo, I., Debey, P. and Rebuffat, S. Structural changes of region 1-16 of the Alzheimer disease Amyloid β -peptide upon zinc binding and *in vitro* aging. *J. Biol. Chem.* 281: 2151-2161 (2006).
17. Chen, Y. and Glabe, C. G. Distinct early folding and aggregation properties of Alzheimer amyloid- β peptides A β 40 and A β 42. *J. Biol. Chem.* 281: 24414-24422 (2006).
18. Harper, J. D., Wong, S. S., Lieber, C. M. and Lansbury, P. T., Jr. Observation of metastable A β amyloid protofibrils by atomic force microscopy. *Chem. Biol.* 4: 119-125 (1997).
19. Bitan, G., Kirkitadze, M. D., Lomakin, A., Vollers, S. S., Benedek, G. B. and Teplow, D. B. Amyloid β -protein (A β) assembly: A β 40 and A β 42 oligomerize through distinct pathways. *Proc. Natl. Acad. Sci. USA.* 100: 330-335 (2003).
20. Williams, A. D., Portellius, E., Kheteroal, I., Guo, J., Cook, K. D., Xu, Y. and Wetzel, R. Mapping A β amyloid fibril secondary structure using scanning proline mutagenesis. *J. Mol. Bio.* 335: 833-842 (2004).
21. Gouras, G. K., Tsai, J., Naslund, J., Vincent, B., Edgar, M., Checler, F., Greenfield, J. P., Haroutunian, V., Buxbaum, J. D., Xu, H., Greengard P. and Relkin, N. R. Intraneuronal A β 42 accumulation in human brain. *Am. J. Pathol.* 156: 15-20 (2000).
22. Zhang, S., Itwata, K., Lachenmann, M. J., Peng, J. W., Li, S., Stimson, E. R., Lu, Y., Felix, A. M., Maggio, J. E. and Lee, J. P. The Alzheimer's peptide A β adopts a collapsed coil structure in water. *J. Struct. Biol.* 130: 130-141 (2000).
23. Walsh, D. M., Klyubin, I., Fadeeva, J. V., Cullen, W. K., Anwyl, R., Wolfe, M. S., Rowan, M. J. and Selkoe, D. J. Naturally secreted oligomers of amyloid β protein potently inhibit hippocampal long-term potentiation *in vivo*. *Nature.* 416: 535-539 (2002).
24. Lesné, S., Koh, M. T., Kotilinek, L., Kaye, R., Glabe, C. G., Yang, A., Gallagher, M. and Ashe, K. H. A specific amyloid- β protein assembly in the brain impairs memory. *Nature.* 440: 352-357 (2006).
25. Walsh, D. M., Tseng, B. P., Rydel, R. E., Podlisny, M. B. and Selkoe, D. J. The oligomerization of amyloid β -protein begins intracellularly in cells derived from human brain. *Biochem.* 39: 10831-10839 (2000).
26. Podlisny, M. B., Ostaszewski, B. L., Squazzo, S. L., Koo, E. H., Rydel, R. E., Teplow, D. B. and Selkoe, D. J. Aggregation of secreted amyloid β -protein into Sodium Dodecyl Sulfate-stable oligomers in cell culture. *J. Biol. Chem.* 270: 9564-9570 (1995).
27. Gong, Y., Chang, L., Viola, K. L., Lacor, P. N., Lambert, M. P., Finch, C. E., Krafft, G. A. and Klein, W. L. Alzheimer's disease-affected brain: presence of oligomeric A β ligands (ADDLs) suggests a molecular basis for reversible memory loss. *Proc. Natl. Acad. Sci. USA.* 100: 10417-10422 (2003).

28. Lashuel, H. A., Hartley, D., Petre, B. M., Walz, T. and Lansbury, P. T., Jr. Amyloid pores from pathogenic mutations. *Nature*. 418: 291 (2002).
29. Teplow, D. B., Lazo, N. D., Bitan, G., Bernstein, S., Wyttenback, T., Bowers, M. T., Baumketner, A., Shea, J., Urbanc, B., Cruz, L., Borreguero, J. and Stanley, H. E. Elucidating amyloid β -protein folding and assembly: a multidisciplinary approach. *Acc. Chem. Res.* 39: 635-645 (2006).
30. Nelson, R. and Eisenberg, D. Structural models of amyloid-like fibrils. *Adv. Protein. Chem.* 73: 235-282 (2006).
31. Kaye, R., Head, E., Thompson, J. L., McIntire, T. M., Milton, S. C., Cotman, C. W. and Glabe, C. G. Common structure of soluble amyloid oligomers implies common mechanism of pathogenesis. *Science*. 300: 486-489 (2003).
32. Crescenzi, O., Tomaselli, S., Guerrini, R., Salvadori, S., D'Ursi, A. M., Temussi, P. A. and Picone, D. Solution structure of the Alzheimer amyloid β -peptide (1-42) in an apolar microenvironment. *Eur. J. Biochem.* 269: 5642-5648 (2002).
33. Kirschner, D. A., Abraham, C. and Selkoe, D. J. X-ray diffraction from intraneuronal paired helical filaments and extraneuronal amyloid fibers in Alzheimer disease indicates cross- β conformation. *Proc. Natl. Acad. Sci. USA*. 83: 503-507 (1986).
34. Petkova, A. T., Ishii, Y., Balbach, J. J., Antzutkin, O. N., Leapman, R. D., Delaglio, F. and Tycko, R. A structural model for Alzheimer's β -amyloid fibrils based on experimental constraints from solid state NMR. *PNAS*. 99: 16742-16747 (2002).
35. Lührs, T., Ritter, C., Adrian, M., Riek-Loher, D., Bohrmann, B., Döbeli, H., Schubert, D. and Riek, R. 3D structure of Alzheimer's amyloid- β (1-42) fibrils. *PNAS*. 102: 17342-17347 (2005).
36. Hardy, J. and Selkoe, D. J. The amyloid hypothesis of Alzheimer's disease: progress and problems on the road to therapeutics. *Science*. 297: 353-356 (2002).
37. Rhodes, G. 2006. 3rd ed., Crystallography made crystal clear, Canada, Academic Press.
38. Sawaya, M. R., Sambashivan, S., Nelson, R., Ivanova, M. I., Sievers, S. A., Apostol, M. I., Thompson, M. J., Balbirnie, M., Wiltzius, J. J. W., McFarlane, H. T., Madsen, A. Ø, Riek, C. and Eisenberg, D. Atomic structures of amyloid cross- β spines reveal varied steric zippers. *Nature*. 447: 453-457 (2007).
39. Buckle, A. M., Zahn, R. and Fersht, A. R. A structural model for GroEL-polypeptide recognition. *Proc. Natl. Acad. Sci. USA*. 94: 3571-3575 (1997).
40. Nelson, R., Sawaya, M. R., Balbirnie, M., Madsen, A. Ø, Riek, C., Grothe, R. and Eisenberg, D. Structure of the cross- β spine of amyloid like fibrils. *Nature*. 435: 773-778 (2005).
41. Braig, K., Otwinowski, Z., Hegde, R., Biosvert, D. C., Joachimiak, A., Horwich, A. L. and Sigler, P. B. The crystal structure of the bacterial chaperonin GroEL at 2.8 Å. *Nature*. 371: 578-586 (1994).
42. Xu, Z., Horwich, A. L. and Sigler, P. B. The crystal structure of the asymmetric GroEL-GroES-(ADP)₇ chaperonin complex. *Nature*. 388: 741-750 (1997).

Websites

43. <http://www.liv.ac.uk/researchintelligence/issue30/alzheimers.html>
44. http://en.wikipedia.org/wiki/Crystal_structure
45. <http://www.jic.ac.uk/staff/david-lawson/xtallog/summary.htm>

Supplements

Supplement 1 Amyloid beta peptide fragment structures

Three structures of amyloid beta fibril-forming segments have been solved with X-ray microcrystallography. These three structures are from two identified fibril-forming segments in the A β peptide. Two structures for the A β peptide fragment MVGGVV (residues 35-40) and one structure for the A β peptide fragment GGVVIA (residues 37-42)³⁸.

The segments form fibrils by the formation of the cross- β structure consisting of a pair of β -sheets. The two β -sheets mate tightly to form a completely dry interface. At the interface the opposing residue side chains interdigitate in a steric zipper³⁸. The side chains form van der Waals interactions because of their shape complementarity⁴⁰. There are variations of the steric-zipper structure, the structures to date fall into five different classes³⁸.

The A β peptide fragment GGVVIA (Fig. S1-1) falls into class 4. GGVVIA forms parallel sheets (the strands in the sheets). The sheets pack with different surfaces adjacent to one another ('face-to-back'). The sheets are oriented antiparallel to one another ('up-down')³⁸.

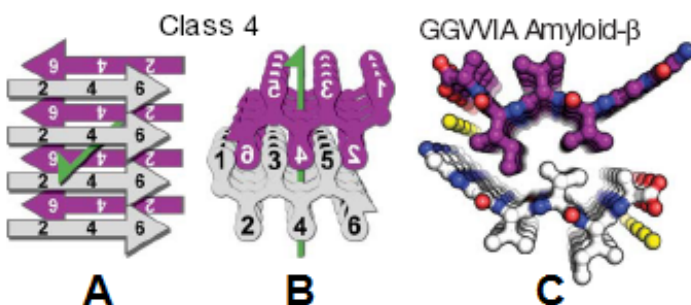


Figure S1-1 GGVVIA microcrystallography structure. (A) and (B) show steric zipper class 4 where GGVVIA belongs. It shows the parallel sheets (the strands in the sheets), the antiparallel orientation of the sheets with respect to one another and the face-to-back orientation. The β -sheets are shown in purple and white. Green arrows show the two-fold screw axis. (C) The atomic resolution structure of GGVVIA showing a two β -sheet motif³⁸.

The A β peptide fragment MVGGVV (Fig. S1-2) falls into class 8. MVGGVV forms antiparallel sheets (the strands in the sheets). The sheets are oriented antiparallel to one another ('up-down'). The MVGGVV segment forms two polymorphs, meaning that it crystallizes in two different forms (Fig. S1-2 C and D)³⁸.

The structures of the different segments are significantly different, suggesting that the fibril of the A β protein could contain more than one type of paired sheets or that the sheet could be built from multiple segments, or perhaps polymorphic fibrils of the same protein exist³⁸.

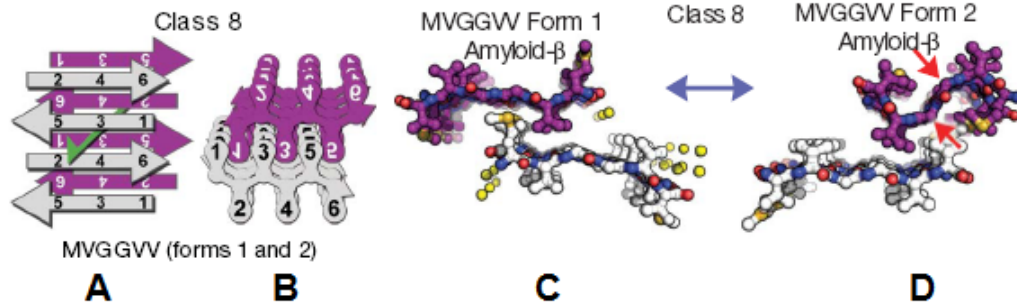


Figure S1-2 MVGGVV microcrystallography structures. (A) and (B) show steric zipper class 8 where MVGGVV belongs. It shows the antiparallel sheets (the strands in the sheets), the antiparallel orientation of the sheets with respect to one another and the face-to-back orientation. The β -sheets are shown in purple and white. Green arrows show the two-fold screw axis. (C) and (D) the atomic resolution structures of the two forms of MVGGVV showing for each form two β -sheet motifs. The red arrows point to the 90° bend in the upper sheet³⁸.

Supplement 2 GroEL background information

GroEL is a chaperonin protein that can be found in the cytoplasm of bacteria, including *E.coli*. Chaperonins are large multisubunit assemblies that mediate ATP-dependent polypeptide chain folding. GroEL has been shown to also facilitate refolding of proteins *in vitro* that would otherwise misfold or aggregate. GroEL requires ATP and the binding of the smaller chaperonin GroES⁴¹.

GroEL is a cylinder composed of two rings of each seven subunits (Fig S2-1 and S2-2). These rings are arranged back-to-back, creating a central cavity (Fig. S2-2). Each subunit consists of three domains (Fig. S2-3). The equatorial domain (residues 6-133 and 409-523) connects the two rings and binds ATP. The intermediate domain (residues 134-190 and 377-408) connects the apical and equatorial domain. The apical domain (residues 191-376) forms the opening of the cylinder and contains the polypeptide and GroES binding sites⁴¹. GroES forms a complex with only one of the two rings, the *cis* ring closing off one of the cavities ends, functioning as a cap (Fig. S2-1)⁴².

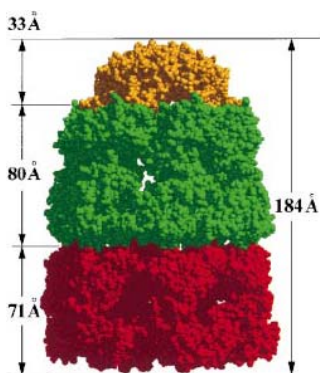


Figure S2-1 GroEL-GroES architecture and lengths. Red = *trans* GroEL ring. Green = *cis* GroEL ring. Gold = GroES⁴².

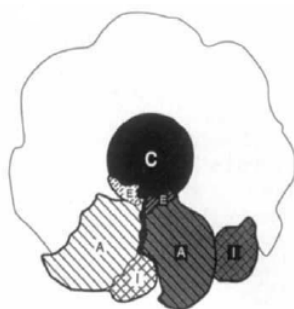


Figure S2-2 Facing into the central cavity. In gray two subunits in the top-ring. A = apical domain. I = intermediate domain. E = equatorial domain. C = central cavity⁴¹.

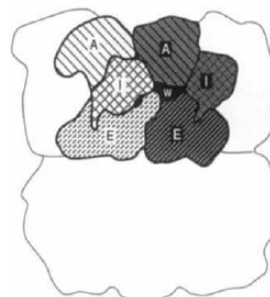


Figure S2-3 The two rings of GroEL arranged back-to-back. In gray two subunits in the top-ring. A = apical domain. I = intermediate domain. E = equatorial domain. W = external opening of a side window⁴¹.

Supplement 3 Chromatogram of a nickel column purification

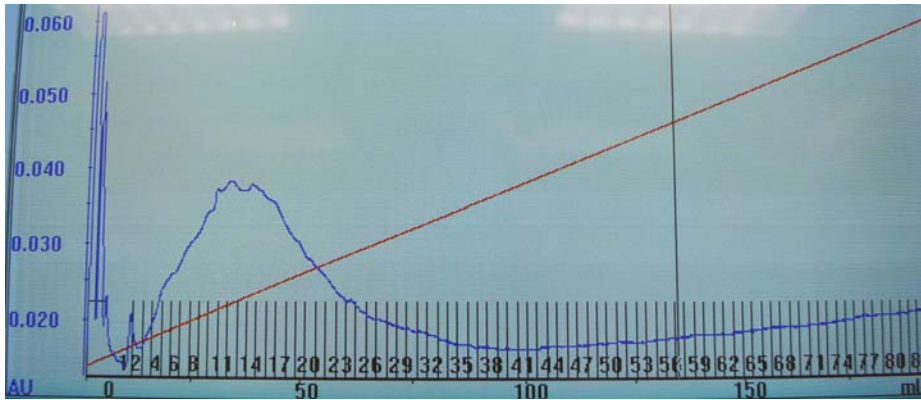


Figure S3-1 Chromatogram of nickel column purification of A376-6MPT-A β 42. Plotted on the y-axis the UV absorbance in absorbance units (AU) and plotted on the x-axis the elution volume (ml) with the fraction numbers. The red line shows the increasing concentration of buffer B.

Supplement 4 Dynamic light scattering analysis

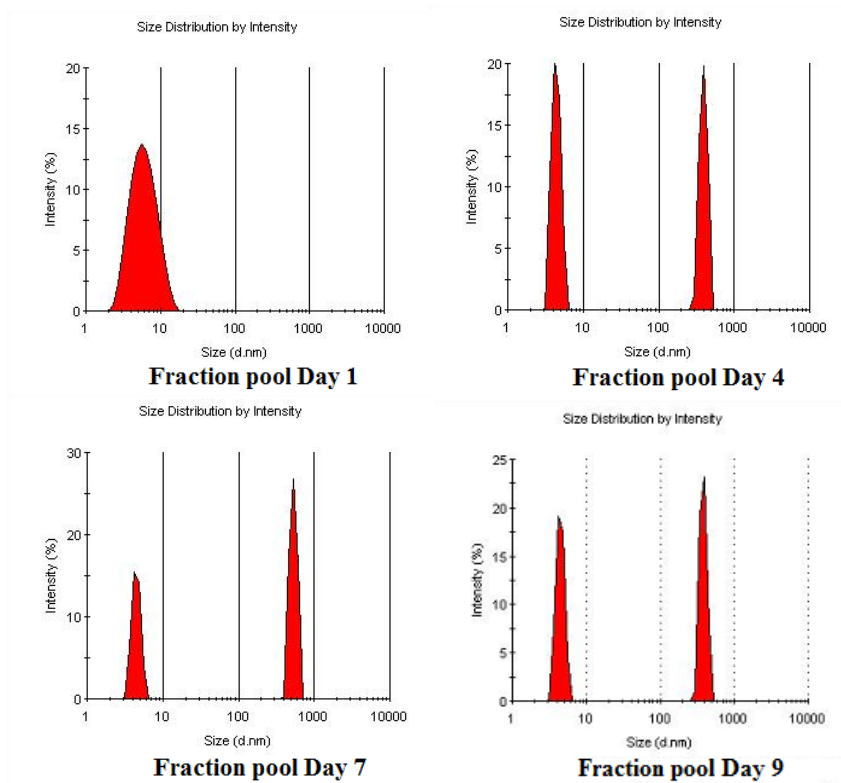


Figure S4-1 Dynamic light scattering of the fraction pool of A336-6SAG-A β 42 at different time points of incubation. On the y-axis is the relative intensity of the scattered light plotted. On the x-axis is the distribution of the different sizes (diameter in nanometer) plotted.

Supplement 5 SDS-PAGE of a size exclusion purification

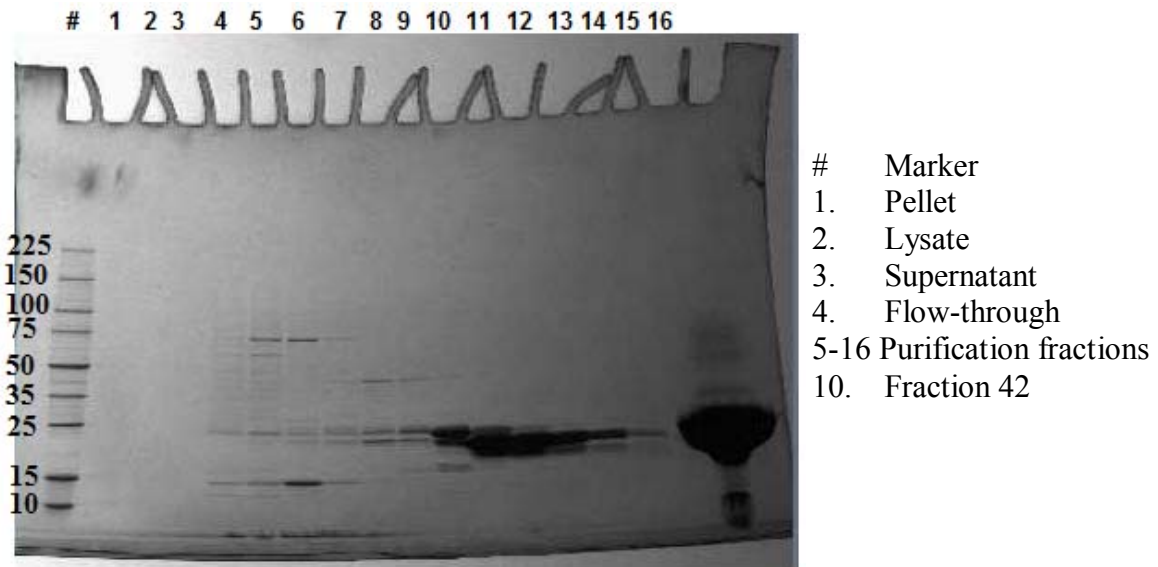


Figure S5-1 SDS-PAGE of a S75 purification of A336-6SAG-A β 42. The last lane contains a protein sample of another experiment.

Supplement 6 Primer nucleotide sequences

Apical forward primer with NdeI restriction site (NdeI apical)

5'-AGC TCA CAT ATG GAA GGT ATG CAG TTC G-3'

T_m = 60.2 °C

Apical 376 reverse primer with NheI restriction site SAG HindIII (Apical 376 NheI)

5'-AGT CAG TAA GCT TAC CAG CAG AGC TAG CAA CGC CGC CTG CTG C-3'

T_m = 70.4 °C

Apical 336 reverse primer with NheI restriction site (Apical 336 NheI)

5'-AGT CAG TAA GCT TAC CAG CAG AGC TAG CCA CGC CAT CGA TGA TAG TGG-3'

T_m = 69.3 °C

Apical 376 reverse primer with XhoI restriction site (Apical 376 XhoI)

5'-GTC GGC CTC GAG TTA AAC GCC GCC TGC-3'

T_m = 68.5 °C

Apical 336 reverse primer with XhoI restriction site (Apical 336 XhoI)

5'-GCT GGC CTC GAG TTA CAC GCC ATC GAT GAT-3'

T_m = 66.3 °C

SAG forward primer (NheI SAG)

5'-CTA GCT CTG CTG GTA-3'

T_m = 46.3

SAGSAG forward primer (NheI SAGSAG)

5'-AGC TTG CCT GCA CTA CCA GCA GAG-3'

T_m = 63.3

SAGSAGSAG forward primer (NheI SAGSAGSAG)

5'-CTA GCT CTG CTG GTA GTG CAG GCA GCG CCG GTA-3'

T_m = 70.5

SAGSAGSAGSAG forward primer (NheI SAGSAGSAGSAG)

5'-CTA GCT CTG CTG GTA GTG CAG GCA GCG CCG GTT CAG CAG GCA-3'

T_m = 74.0

MPTATA forward primer (NheI MPTATA)

5' CTA GCA TGC CTA CTG CTA CTG CTA-3'

T_m = 58.0

NSQPNTNGS forward primer (NheI NSQPNTNGS)

5'-CTA GCA ATT CTC AAC CTA ATA CTA ATG GTT CTA-3'

T_m = 56.2

NSSGSGSNSSGS forward primer (NheI NSSGSGSNSSGS)

5'-CTA GCA ATT CTT CCG GTA GCG GTA GTA ACT CGT CAG GTA GTA-3'

T_m = 65.3

Aβ 1-42 forward primer with HindIII restriction site (HindIII Aβ1-42)

5'-CAC TGA GTA AGC TTG ATG CAG AAT TCC G-3'

T_m = 59.5 °C

Aβ 17-42 forward primer with HindIII restriction site (HindIII Aβ17-42)

5'-AGT CAG AAG CTT TTG GTG TTC TTT GCA GAA G-3'

T_m = 60.9 °C

Supplement 7 Linker nucleotide sequences

SAG forward linker:

5'-CTA GCT CTG CTG GTA-3'

T_m = 46.3 °C

SAG reverse linker:

5'-AGC TTA CCA GCA GAG-3'

T_m = 47.4 °C

SAGSAG forward linker:

5'-CTA GCT CTG CTG GTA GTG CAG GCA-3'

T_m = 62.6 °C

SAGSAG reverse linker:

5'-AGC TTG CCT GCA CTA CCA GCA GAG-3'

T_m = 63.3 °C

SAGSAGSAG forward linker:

5'-CTA GCT CTG CTG GTA GTG CAG GCA GCG CCG GTA-3'

T_m = 70.5 °C

SAGSAGSAG reverse linker:

5'-AGC TTA CCG GCG CTG CCT GCA CTA CCA GCA GAG-3'

T_m = 71.0 °C

SAGSAGSAGSAG forward linker:

5'-CTA GCT CTG CTG GTA GTG CAG GCA GCG CCG GTT CAG CAG GCA-3'

T_m = 74.0 °C

SAGSAGSAGSAG reverse linker:

5'-AGC TTG CCT GCT GAA CCG GCG CTG CCT GCA CTA CCA GCA GAG-3'

T_m = 74.4 °C

MPTATA forward linker:

5' CTA GCA TGC CTA CTG CTA CTG CTA-3'

T_m = 58.0 °C

MPTATA reverse linker:

5'-AGC TTA GCA GTA GCA GTA GGC ATG-3'

T_m = 58.7 °C

NSQPNTNGS forward linker:

5'-CTA GCA ATT CTC AAC CTA ATA CTA ATG GTT CTA-3'

T_m = 56.2 °C

NSQPNTNGS reverse linker:

5'-AGC TTA GAA CCA TTA GTA TTA GGT TGA GAA TTG-3'

$T_m = 56.6 \text{ }^\circ\text{C}$

NSSGSGSNSSGS forward linker:

5'-CTA GCA ATT CTT CCG GTA GCG GTA GTA ACT CGT CAG GTA GTA-3'

$T_m = 65.3 \text{ }^\circ\text{C}$

NSSGSGSNSSGS reverse linker:

5'-AGC TTA CTA CCT GAC GAG TTA CTA CCG CTA CCG GAA GAA TTG-3'

$T_m = 65.7 \text{ }^\circ\text{C}$

Supplement 8 Amino acids sequence constructs

A376-SAG-A β 42

sequence confirmed 10-23-08

Expected MW

28081 Da uncleaved
23566.9 Da without A β 1-42
25386.1 Da without His-tag
20872 Da without His-tag and A β 1-42

Amino acid sequence

M G S S H H H H H S G L Q G Y R E P V L P G H His-tag 2694.9 Da

**M E G M Q F D R G Y L S P Y F I N K P E T G A V E L E S P F I L L A D K K I S N I
R E M L P V L E A V A K A G K P L L I I A E D V E G E A L A T L V V N T M R G
I V K V A A V K A P G F G D R R K A M L Q D I A T L T G G T V I S E E I G M E L
E K A T L E D L G Q A K R V V I N K D T T T I I D G V G E E A A I Q G R V A Q I
R Q Q I E E A T S D Y D R E K L Q E R V A K L A G G V**

M + apical 191-376 20239.3 Da

A S S A G K L

Linker and restriction sites 632.7 Da

**D A E F R H D S G Y E V H H Q K L V F F A E D V G S N K G A I I G L M V G G V
V I A**

A β 1-42 4514.1 Da

Extinction coefficient: 7450

A376-6SAG-A β 42

sequence confirmed 03-18-08

Expected MW

28296.2 uncleaved
23782.1 Da without A β 1-42
25601.3 Da without His-tag
21087.2 Da without His-tag and A β 1-42

Amino acid sequence

M G S S H H H H H S G L Q G Y R E P V L P G H His-tag 2694.9 Da

**M E G M Q F D R G Y L S P Y F I N K P E T G A V E L E S P F I L L A D K K I S N I
R E M L P V L E A V A K A G K P L L I I A E D V E G E A L A T L V V N T M R G
I V K V A A V K A P G F G D R R K A M L Q D I A T L T G G T V I S E E I G M E L
E K A T L E D L G Q A K R V V I N K D T T T I I D G V G E E A A I Q G R V A Q I
R Q Q I E E A T S D Y D R E K L Q E R V A K L A G G V**

M + apical 191-376 20239.3 Da

A S S A G S A G K L

Linker and restriction sites 847.9 Da

D A E F R H D S G Y E V H H Q K L V F F A E D V G S N K G A I I G L M V G G V
V I A A β 1-42 4514.1 Da

Extinction coefficient: 7450

A376-9SAG-A β 42

sequence confirmed 04-02-08

Expected MW

28457.4 Da uncleaved

23943.3 Da without A β 1-42

25762.5 Da without His-tag

21248.4 Da without His-tag and A β 1-42

Amino acid sequence

M G S S H H H H H S G L Q G Y R E P V L P G H

His-tag 2694.9 Da

**M E G M Q F D R G Y L S P Y F I N K P E T G A V E L E S P F I L L A D K K I S N I
R E M L P V L E A V A K A G K P L L I I A E D V E G E A L A T L V V N T M R G
I V K V A A V K A P G F G D R R K A M L Q D I A T L T G G T V I S E E I G M E L
E K A T L E D L G Q A K R V V I N K D T T T I I D G V G E E A A I Q G R V A Q I
R Q Q I E E A T S D Y D R E K L Q E R V A K L A G G V**

M + apical 191-376 20239.3 Da

A S S A G S A G S A G K L

Linker and restriction sites 1162.2 Da

D A E F R H D S G Y E V H H Q K L V F F A E D V G S N K G A I I G L M V G G V
V I A A β 1-42 4514.1 Da

Extinction coefficient: 7450

A376-12SAG-A β 42

sequence confirmed 04-03-08

Expected MW

28573.5 Da uncleaved

24059.4 Da without A β 1-42

25878.6 Da without His-tag

21364.5 Da without His-tag and A β 1-42

Amino acid sequence

M G S S H H H H H S G L Q G Y R E P V L P G H

His-tag 2694.9 Da

MEGMQFDRGYLSPYFINKPETGAVELESPFILLADKKISNI
REMLPVL EAVAKAGKPLLIIAEDVEGEALATLVVNTMRG
IVKVA AVKAPGFGDRRKAMLQDIATLTGGT VISEEIGMEL
EKATLEDLGQAKRVVINKDTTTTIIDGVGEEAAIQGRVAQI
RQQIEEATSDYDREKLQERVAKLAGG

M + apical 191-376 20239.3 Da

ASSAGSAGSAGSAGKL

Linker and restriction sites 1278.3 Da

DAEFRHDSGYEVHHQKLVFFAEDVGSNKGAIIGLMVGGV
VIA

Aβ 1-42 4514.1 Da

Extinction coefficient: 7450

A376-6MPT-Aβ42

sequence confirmed 03-10-08

Expected MW

28438.4 Da uncleaved
23924.3 Da without Aβ1-42
25743.5 Da without His-tag
21229.4 Da without His-tag and Aβ1-42

Amino acid sequence

MGSSHHHHHSSGLQGYREPVLPGH

His-tag 2694.9 Da

MEGMQFDRGYLSPYFINKPETGAVELESPFILLADKKISNI
REMLPVL EAVAKAGKPLLIIAEDVEGEALATLVVNTMRG
IVKVA AVKAPGFGDRRKAMLQDIATLTGGT VISEEIGMEL
EKATLEDLGQAKRVVINKDTTTTIIDGVGEEAAIQGRVAQI
RQQIEEATSDYDREKLQERVAKLAGGV

M + apical 191-376 20239.3 Da

ASMPATAK L

Linker and restriction sites 990.1 Da

DAEFRHDSGYEVHHQKLVFFAEDVGSNKGAIIGLMVGGV
VIA

Aβ 1-42 4514.1 Da

Extinction coefficient: 7450

A376-9NSQ-Aβ42

sequence confirmed 04-02-08

Expected MW

28711.7 Da uncleaved
24197.6 Da without Aβ1-42

26016.8 Da without His-tag
21502.7 Da without His-tag and A β 1-42

Amino acid sequence

MGSSHHHHHSSGLQGYREPVLPGH His-tag 2694.9 Da

**MEGMQFDRGYLSPYFINKPETGAVELESPFILLADKKISNI
REMLPVLEAVAKAGKPLLIIAEDVEGEALATLVVNTMRG
IVKVA AVKAPGFGDRRKAMLQDIATLTGGTWISEEIGMEL
EKATLEDLGQAKRVVINKDTTTIIDGVGEEAAIQGRVAQI
RQQIEEATSDYDREKLQERVAKLAGG**

M + apical 191-376 20239.3 Da

ASNSQPNTNGSKL Linker and restriction sites 1317.3 Da

**DAEFRHDSGYEVHHQKLVFFAEDVGSNKGAIIGLMVGGV
VIA** A β 1-42 4514.1 Da

Extinction coefficient: 7450

A376-12NSS-A β 42

sequence confirmed 04-02-08

Expected MW

28721.6 Da uncleaved
24207.5 Da without A β 1-42
26026.7 Da without His-tag
21512.6 Da without His-tag and A β 1-42

Amino acid sequence

MGSSHHHHHSSGLQGYREPVLPGH His-tag 2694.9 Da

**MEGMQFDRGYLSPYFINKPETGAVELESPFILLADKKISNI
REMLPVLEAVAKAGKPLLIIAEDVEGEALATLVVNTMRG
IVKVA AVKAPGFGDRRKAMLQDIATLTGGTWISEEIGMEL
EKATLEDLGQAKRVVINKDTTTIIDGVGEEAAIQGRVAQI
RQQIEEATSDYDREKLQERVAKLAGG**

M + apical 191-376 20239.3 Da

ASNSSGSGSNSSGSKL Linker and restriction sites 1426.4 Da

**DAEFRHDSGYEVHHQKLVFFAEDVGSNKGAIIGLMVGGV
VIA** A β 1-42 4514.1 Da

Extinction coefficient: 7450

A376-6SAG-A β 17-42**sequence confirmed 01-24-08****Expected MW**

26359.1 Da uncleaved
 23782.1 Da without A β 17-42
 23664.2 Da without His-tag
 21087.2 Da without His-tag and A β 17-42

Amino acid sequence

M G S S H H H H H S G L Q G Y R E P V L P G H His-tag 2694.9 Da

**M E G M Q F D R G Y L S P Y F I N K P E T G A V E L E S P F I L L A D K K I S N I
 R E M L P V L E A V A K A G K P L L I A E D V E G E A L A T L V V N T M R G
 I V K V A A V K A P G F G D R R K A M L Q D I A T L T G G T V I S E E I G M E L
 E K A T L E D L G Q A K R V V I N K D T T T I I D G V G E E A A I Q G R V A Q I
 R Q Q I E E A T S D Y D R E K L Q E R V A K L A G G V**

M + apical 191-376 20239.3 Da**A S S A G S A G K L**Linker and restriction sites 847.9 Da**L V F F A E D V G S N K G A I I G L M V G G V V I A** A β 17-42 2577.0 Da

Extinction coefficient: 5960

A336-6SAG-A β 42**sequence confirmed 01-24-08****Expected MW**

23900.4 Da uncleaved
 19386.3 Da without A β 1-42
 21205.5 Da without His-tag
 16691.4 Da without His-tag and A β 1-42

Amino acid sequence

M G S S H H H H H S G L Q G Y R E P V L P G H His-tag 2694.9 Da

**M E G M Q F D R G Y L S P Y F I N K P E T G A V E L E S P F I L L A D K K I S N I
 R E M L P V L E A V A K A G K P L L I A E D V E G E A L A T L V V N T M R G
 I V K V A A V K A P G F G D R R K A M L Q D I A T L T G G T V I S E E I G M E L
 E K A T L E D L G Q A K R V V I N K D T T T I I D G V**

M + apical 191-336 15843.5 Da**A S S A G S A G K L**Linker and restriction sites 847.9 Da

**D A E F R H D S G Y E V H H Q K L V F F A E D V G S N K G A I I G L M V G G V
 V I A** A β 1-42 4514.1 Da

Extinction coefficient: 5960

A336-6SAG-A β 17-42

sequence confirmed 01-24-08

Expected MW

21963.3 Da uncleaved
19386.3 Da without A β 17-42
19268.4 Da without His-tag
16691.4 Da without His-tag and A β 17-42

Amino acid sequence

M G S S H H H H H S G L Q G Y R E P V L P G H His-tag 2694.9 Da

**M E G M Q F D R G Y L S P Y F I N K P E T G A V E L E S P F I L L A D K K I S N I
R E M L P V L E A V A K A G K P L L I I A E D V E G E A L A T L V V N T M R G
I V K V A A V K A P G F G D R R K A M L Q D I A T L T G G T V I S E E I G M E L
E K A T L E D L G Q A K R V V I N K D T T T I I D G V**

M + apical 191-336 15843.5 Da

A S S A G S A G K L

Linker and restriction sites 847.9 Da

L V F F A E D V G S N K G A I I G L M V G G V V I A

A β 17-42 2577.0 Da

Extinction coefficient: 4470

A336-12GSA-A β 42

sequence confirmed 02-20-08

Expected MW

24290.8 Da uncleaved
19776.7 Da without A β 1-42
21595.9 Da without His-tag
17081.8 Da without His-tag and A β 1-42

Amino acid sequence

M G S S H H H H H S G L Q G Y R E P V L P G H His-tag 2694.9 Da

**M E G M Q F D R G Y L S P Y F I N K P E T G A V E L E S P F I L L A D K K I S N I
R E M L P V L E A V A K A G K P L L I I A E D V E G E A L A T L V V N T M R G
I V K V A A V K A P G F G D R R K A M L Q D I A T L T G G T V I S E E I G M E L
E K A T L E D L G Q A K R V V I N K D T T T I I D G V**

M + apical 191-336 15843.5 Da

G S A G S A A G S G E F K L

Linker and restriction site 1238.3 Da

DAEFRHDSGYEVHHQKLVFFAEDVGSNKGAIIGLMVGGV
VIA Aβ 1-42 4514.1 Da

Extinction coefficient: 5960

A376 control

sequence confirmed 04-02-08

Expected MW

22916.2 Da uncleaved

20221.3 Da without His-tag

Amino acid sequence

MGSSHHHHHHSGLQGYREPVLPGH

His-tag 2694.9 Da

MEGMQFDRGYLSPYFINKPETGAVELESPFILLADKKISNI
REMLPVLEAVAKAGKPLLIIAEDVEGEALATLVVNTMRG
IVKVA AVKAPGFGDRRKAMLQDIATLTGGTWISEEIGMEL
EKATLEDLGQAKRVVINKDTTTIIDGVGEEAAIQGRVAQI
RQQIEEATSDYDREKLRVAKLAGGV

M + apical 191-376 20239.3 Da

Extinction coefficient: 5960

A336 control

sequence confirmed 04-02-08

Expected MW

18520.4 Da uncleaved

15825.5 Da without His-tag

Amino acid sequence

MGSSHHHHHHSGLQGYREPVLPGH

His-tag 2694.9 Da

MEGMQFDRGYLSPYFINKPETGAVELESPFILLADKKISNI
REMLPVLEAVAKAGKPLLIIAEDVEGEALATLVVNTMRG
IVKVA AVKAPGFGDRRKAMLQDIATLTGGTWISEEIGMEL
EKATLEDLGQAKRVVINKDTTTIIDGV

M + apical 191-336 15843.5 Da

Extinction coefficient: 4470